arXiv:2312.02826v1 [cs.LG] 5 Dec 2023

CALIBRATED ADAPTIVE TEACHER FOR DOMAIN ADAPTIVE INTELLIGENT FAULT DIAGNOSIS

Florent Forest
Intelligent Maintenance and Operations Systems
EPFL
Lausanne, Switzerland
florent.forest@epfl.ch

Olga Fink
Intelligent Maintenance and Operations Systems
EPFL
Lausanne, Switzerland
olga.fink@epfl.ch

ABSTRACT

Intelligent Fault Diagnosis (IFD) based on deep learning has proven to be an effective and flexible solution, attracting extensive research. Deep neural networks are able to learn rich representations from vast amounts of representative labeled data for various applications. In IFD, they can achieve high classification performance from signals in an end-to-end manner, without the need for extensive domain knowledge. However, deep learning models usually only perform well on the data distribution they have been trained on. When applied to a different distribution, they may experience a severe performance drop. This is also observed in fault diagnosis, where the assets are often operated in working conditions different from the ones in which the labeled data have been collected. This challenge has been addressed recently by Domain Adaptation approaches for IFD. In particular, unsupervised domain adaptation (UDA) deals with the scenario where labeled data are available in a source domain, and only unlabeled data are available in a target domain, where domains may correspond to different operating conditions. Recent methods have relied on training with confident pseudo-labels for the unlabeled target samples. However, the confidence-based selection of pseudo-labels is hindered by poorly calibrated confidence estimates in the target domain, primarily due to over-confident predictions, which limits the quality of pseudo-labels and leads to error accumulation. In this paper, we propose a novel UDA method called Calibrated Adaptive Teacher (CAT), where we propose to calibrate the predictions of the teacher network on target samples throughout the self-training process, leveraging well-known post-hoc calibration techniques such as temperature scaling. We evaluate CAT on domain-adaptive IFD and perform extensive experiments on the Paderborn University benchmark dataset for fault diagnosis of rolling bearings under varying operating conditions using both time-domain and frequency-domain inputs. Our proposed method achieves state-of-the-art performance on the majority of transfer tasks.

***K*eywords** Intelligent Fault Diagnosis · Unsupervised Domain Adaptation · Self-training · Pseudo-labels · Mean Teacher · Calibration

1 Introduction

Fault diagnosis of industrial equipment is a crucial task in Prognostics and Health Management. Intelligent Fault Diagnosis (IFD) based on deep learning has proven to be an effective and flexible solution, attracting extensive research [1, 2]. Deep neural networks are able to learn rich representations from extensive labeled data, allowing them to tackle various tasks across different applications. In IFD in particular, they can achieve high classification performance from sensor data such as time series or spectrograms in an end-to-end manner, without the need for incorporating extensive domain knowledge. However, deep learning models usually only perform well on the data distribution they have been trained on. When applied to a different distribution, they may experience a severe performance drop. This is also observed in fault diagnosis, where the industrial assets are often operated in working conditions different from those in which the labeled data have been collected. Furthermore, obtaining labeled data is difficult and costly in real-world

industrial settings. This challenge has recently been addressed recently by Deep Transfer Learning (DTL) and Domain Adaptation (DA) approaches for IFD [3, 4].

Domain adaptation [5] is a type of transfer learning approach aiming at adapting a model from a source domain to a different but related target domain. In particular, unsupervised domain adaptation (UDA) addresses the setting where labeled data are available in the source domain and only unlabeled data are available in the target domain. The discrepancy between the domains is referred to as domain shift. In the context of fault diagnosis, adaptation can be performed between different operating conditions [6, 7], units of a fleet [8, 9, 10, 11], from laboratory to real-world equipment [12] or from synthetic or simulated data to real data [13, 14]. Prevailing approaches for UDA focus on reducing the discrepancy between domains and learning domain-invariant features using the maximum mean discrepancy (MMD) [15], maximum classifier discrepancy (MCD) [16], optimal transport [17] or domain-adversarial training [18]. The latter approach is at the core of domain-adversarial neural networks (DANN) [18], and has been applied extensively for fault diagnosis [10, 19, 11].

Self-training [20] has emerged as an effective alternative for domain adaptation. First introduced for semi-supervised learning, self-training consists in iteratively generating a set of pseudo-labels [21] on the unlabeled data and retraining the network under the supervision of these pseudo-labels [22, 23, 24]. However, noisy and inaccurate pseudo-labels hurt the training process. To address this issue, only the most confident predictions are selected for pseudo-labeling, typically using prediction confidence (i.e., the maximum softmax probability) as a proxy for correctness. Curriculum pseudo-labeling (CPL) [25] is a strategy where pseudo-labels are gradually introduced during the learning process in an "easy-to-hard" manner, starting with the most confident target predictions. Once the model is adapted to the target domain, additional samples can be explored. Confident predictions can be selected using a fixed confidence threshold [26] or an adaptive threshold that dynamically adjusts for each class during training to consider the varying difficulties of classes and enable target samples from low-confidence classes to participate early in the training [27, 25]. Alternatively, pseudo-labels can be selected by fixing a proportion of the most confident predictions for each class instead of using an explicit threshold value [28, 29]. In [30], the variance of predictions between two network sub-branches is used as a replacement for prediction confidence to estimate uncertainty. In their study, French *et al.* [31] state that the confidence thresholding stabilizes the training and acts as filter to increase the number of correct pseudo-labels.

Two main challenges arise in self-training algorithms [32]: (1) Choosing a trustworthy proxy measure of classification accuracy on unlabeled data and (2) Selecting a threshold on this measure for pseudo-labeling at each training iteration. While solutions have been proposed to tackle the second challenge in the previously discussed literature, in the form of adaptive thresholds capable of handling varying class difficulties during training, the first challenge has remained unaddressed. In this work, we address the first challenge, which is related to uncertainty estimation and model calibration. It is well-known that deep neural networks are often badly calibrated and produce overconfident outputs, even for incorrect predictions [33, 34, 35]. Furthermore, in presence of a domain shift, the calibration of a model trained on the source domain will degrade even more in the target domain due to the distribution shift [36, 37]. In self-training algorithms for domain adaptation, the confidence-based selection of pseudo-labels is hindered by poorly calibrated confidence estimates in the target domain. This limitation restricts the quality of pseudo-labels and leading to error accumulation.

In recent literature, various applications of UDA methods for deep learning-based intelligent fault diagnosis have been explored [3, 4]. The main directions explored include domain-adversarial training [38, 39, 40, 41], MMD [42, 43] and MCD [44]. Among all possible methods, DANN is established as a strong baseline on most benchmark datasets [3]. Self-training UDA methods based on pseudo-labeling of target samples, which are the main focus of this study, have also been explored in the literature. Prediction Consistency Guided Convolutional Neural Networks (PCG-CNN) [45] draws direct inspiration from [31] and uses a Mean Teacher with a consistency loss, a fixed confidence threshold of 0.96 and a class balance loss. The deep transfer learning with improved pseudo-label learning method (DTL-IPLL) [46] combines MK-MMD feature alignment and pseudo-labeling with a class-wise adaptive threshold as well as a "making decision-twice" strategy, i.e. predicting twice and discarding the predictions if they differ (which is similar in spirit to Monte-Carlo Dropout [47]). Wang *et al.* [48] proposed to achieve joint distribution alignment by combining marginal alignment using DAN with Wasserstein distance and conditional alignment using a triplet loss, using pseudo-labels for target samples. Pseudo-labels are also selected using CPL with a dynamic adaptive threshold. The Contrastive Cluster Center (CCC) [49] approach involves a combination of adversarial training, contrastive cluster alignment and pseudo-labeling, where pseudo-labels of target samples far away from cluster centers are filtered out, but this method is not using self-training. In the semi-supervised learning setting, [50] uses an aggregation of indicators among which the entropy on unlabeled samples. Pseudo-labels can also be obtained in an unsupervised way through clustering [51]. Differently, [52] uses a prototypical network and filters the pseudo-labels using a confidence threshold based on Monte-Carlo Dropout uncertainty. Finally, [53] propose to gradually enlarge the set of selected pseudo-labels by using the Euclidean distance in feature space as a measure of confidence, and assigns pseudo-labels using a nearest-neighbor

classifier instead of directly predicting with the classifier itself. However, none of these works has addressed the challenge of the calibration of confidence estimates for selecting pseudo-labels in the target domain.

In this paper, we propose a novel UDA method called Calibrated Adaptive Teacher (CAT). The primary novelty of the proposed approach is in improving the calibration in the target domain, with the goal of increasing the accuracy of selected pseudo-labels. CAT consists in a cross-domain teacher-student architecture, where the student network receives confident target pseudo-labels from the teacher network, which is in turn updated by an exponential moving average of the student's weights. Domain-adversarial feature learning is leveraged to alleviate the domain gap. This architecture is based upon the Adaptive Teacher (AT) [54], recently introduced for object detection in computer vision, and has never been applied to IFD yet. To address the issue of target-domain calibration, we propose to calibrate the predictions of the teacher network on target samples throughout the self-training process, using post-hoc calibration techniques such as temperature scaling [33]. We apply our proposed method to domain-adaptive intelligent fault diagnosis and perform extensive benchmarks and ablation studies on the Paderborn University (PU) bearing dataset, which is characterized by large domain gaps and provides challenging transfer tasks between operating conditions. Experiments are carried out on time-domain and frequency-domain (Fourier transform) inputs, following the benchmark setup by [3]. We demonstrate state-of-the-art performance on most transfer tasks both with time-domain and frequency-domain inputs.

The main contributions of this paper are summarized as follows:

1. We propose a novel unsupervised domain adaptation approach, Calibrated Adaptive Teacher (CAT), aiming to improve the calibration of pseudo-labels in the target domain, and thus, the overall accuracy on the target data. Our approach consists in introducing post-hoc calibration of the teacher predictions during the training.
2. We evaluate our approach on intelligent fault diagnosis and conduct extensive studies on the Paderborn University (PU) bearing dataset, with both time-domain and frequency-domain inputs.
3. CAT significantly outperforms previous approaches in terms of accuracy on most transfer tasks, and effectively reduces the calibration error in target domain, leading to an increased target accuracy.
4. We compare four different post-hoc calibration techniques, and demonstrate that temperature scaling [33] and CPCS [36] are the most effective calibration strategies.

The remainder of the paper is organized as follows. In Section 2, we provide technical background required before introducing the details of our method in Section 3. Then, we present experimental settings and results in Section 4. Finally, Section 6 concludes this paper.

2 Background

2.1 Notations

We will use the following notations throughout the paper. Since fault diagnostics can be defined as classification problems, we consider K-class classification tasks whereby each class is typically associated with a different fault type. The source (S) and target (T) data are split into training and test sets, with samples and labels respectively denoted by $\mathbf{X}^{\mathrm{S}}_{\mathrm{train}}$, $\mathbf{Y}^{\mathrm{S}}_{\mathrm{train}}$, $\mathbf{X}^{\mathrm{S}}_{\mathrm{test}}$, $\mathbf{Y}^{\mathrm{S}}_{\mathrm{test}}$ and $\mathbf{X}^{\mathrm{T}}_{\mathrm{train}}$. In the UDA setting, no labels are available in the target domain. The target training labels $\mathbf{Y}^{\mathrm{T}}_{\mathrm{train}}$ and target test set $\mathbf{Y}^{\mathrm{T}}_{\mathrm{test}}$, $\mathbf{Y}^{\mathrm{T}}_{\mathrm{test}}$ are used for evaluation purpose only.

2.2 Domain-Adversarial Neural Networks (DANN)

Domain-adversarial neural networks (DANN) [18] have emerged as one of the most prominent approaches in UDA. Typically, DANN comprise a feature encoder, a task-specific module (e.g., a classification head as in our case), and a domain classifier, also referred to as discriminator. The feature encoder is shared between the classifier and the discriminator. The underlying principle of this methodology is to train the discriminator to classify the input sample features as belonging to either the source or the target domain. While the discriminator is trained to minimize its classification error, the feature encoder tries to generate indistinguishable features to fool the discriminator, hence the term *adversarial*. This is commonly achieved using a gradient reversal layer (GRL) [18]. As a result, the marginal distributions of source and target features become aligned, ultimately improving the performance of the source-trained classifier. Domain-adversarial training occurs concurrently with the training of the main task.

2.3 Mean and Adaptive Teacher

Mean Teacher [55] is a variant of temporal ensembling [56] approach originally proposed for semi-supervised learning, where knowledge is distilled from a teacher network into a student network. The student is trained with standard

gradient updating, whereas the teacher is gradually updated through an exponential moving average (EMA) of the student weights, resulting in an ensemble of all the previous iterations of the student network, increasing its robustness to inaccurate and noisy predictions on unlabeled data. The knowledge distillation can be achieved via a consistency loss between the teacher's and student's predicted probabilities, or via hard pseudo-labeling of the unlabeled samples by the teacher with a confidence threshold to increase the number of correct labels from the teacher used in the student's learning. Mean Teacher was extended to domain adaptation in [31], using a consistency loss on predicted target probabilities and a confidence threshold, as well as a class balance loss to minimize the binary cross entropy between the mean target class probabilities and a uniform distribution. The confidence threshold is proposed as a replacement to the Gaussian ramp-up used in [56, 55], to stabilize the training and act as filter to increase the number of correct pseudo-labels from the teacher used in the student's learning.

Adaptive Teacher (AT) [54] was recently proposed to extend the semi-supervised learning Mean Teacher-based method Unbiased Teacher [57] for UDA in object detection. AT basically combines DANN and Unbiased Teacher into a single architecture (see Figure 1). Concretely, a domain discriminator is added to the student network to perform feature alignment jointly with mutual teacher-student learning. In AT, the teacher provides hard pseudo-labels of target samples that are filtered using a fixed confidence threshold. Then, the cross-domain student network is trained simultaneously on the labeled source data and the pseudo-labeled target data.

2.4 Model calibration

Classification models typically output conditional probabilities for each class given an input sample $\mathbf{x}_i$ by applying a softmax activation on the logits: $\mathbf{p}_i = \sigma(\mathbf{z}_i)$. The predicted class is $\hat{y}_i = \arg\max_y \mathbf{p}_i[y]$, and its corresponding probability is called prediction confidence:

$$c_i := \max \mathbf{p}_i = \mathbf{p}_i[\hat{y}_i]. \tag{1}$$

A classifier is said to be *well-calibrated* if the confidence estimates are equal to the true accuracy of the predictions. For instance, if the confidence is equal to 0.9, the prediction should be correct 90 percent of the time. The calibration of a model can be represented visually by a reliability diagram [58, 33], plotting the expected accuracy as a function of average confidence (see e.g., Figure 3). In order to estimate these quantities from a finite data set, we divide the $[0, 1]$ interval into M equally-spaced bins of size $1/M$, and partition the samples into groups $B_m := \{i \; ; \; \frac{m-1}{M} < c_i \leq \frac{m}{M}, 1 \leq m \leq M\}$. Then, we define the expected accuracy and average confidence of a bin as follows:

$$\text{acc}(B_m) := \frac{1}{|B_m|} \sum_{i \in B_m} \mathbb{1}(\hat{y}_i = y_i) \tag{2}$$

$$\text{conf}(B_m) := \frac{1}{|B_m|} \sum_{i \in B_m} c_i. \tag{3}$$

where y_i is the true label and $\mathbb{1}$ is the indicator function equal to 1 when its argument is true and 0 otherwise. In a perfectly calibrated model, these quantities are supposed to be equal. Whenever we have $\text{acc}(B_m) < \text{conf}(B_m)$, the model is said to be *over-confident*, and in the opposite case, it is said to be *under-confident*. Hence, a well-calibrated model should produce a reliability diagram close to the diagonal. To summarize the calibration quality, a commonly used metric is the Expected Calibration Error (ECE) [59], i.e.:

$$\text{ECE} := \sum_{m=1}^{M} \frac{|B_m|}{N} |\text{acc}(B_m) - \text{conf}(B_m)| \tag{4}$$

where N is the total number of samples.

While a well-calibrated model is desirable, it was shown empirically that neural networks are often badly calibrated in classification [33], regression [34] and anomaly detection [35]. In response, several techniques for network calibration have been developed, which can be broadly classified into *post-hoc*, *train-time*, and through *out-of-distribution detection* [60]. Additionally, it was also demonstrated that calibration degrades under domain shift [61]. Thus, in the setting of UDA, models are poorly calibrated in the target domain [37]. In this paragraph, we briefly introduce the post-hoc calibration techniques for multi-class classification used in our work.

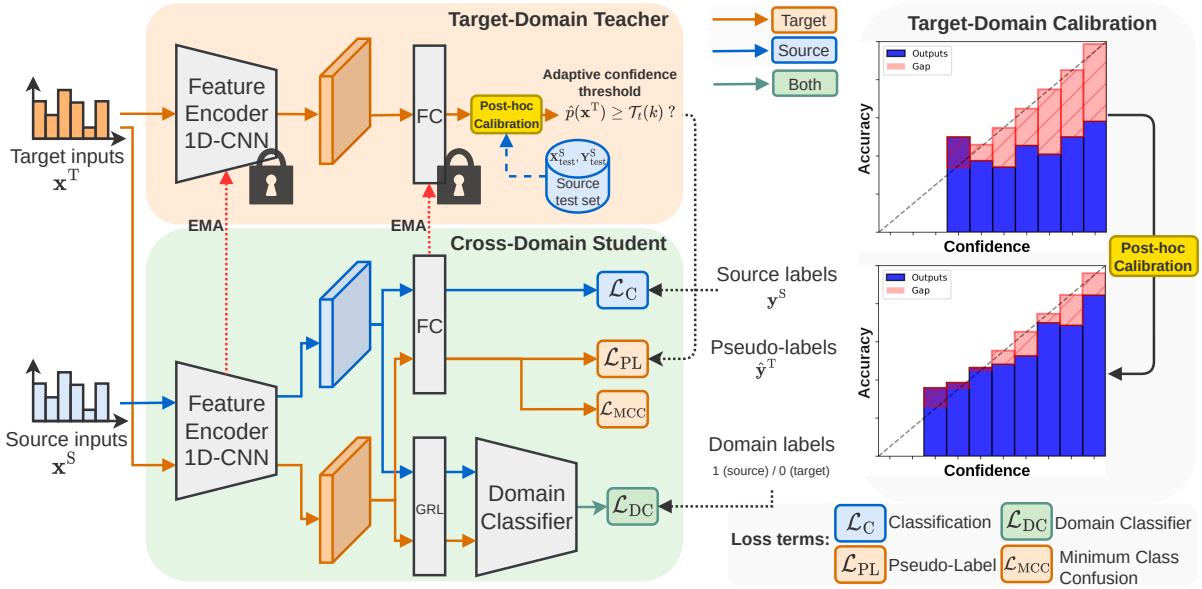

Figure 1: Our proposed Calibrated Adaptive Teacher (CAT). The main novelty involves a post-hoc calibration of the teacher predictions in the target domain throughout the self-training process, improving the quality of pseudo-labels.

Temperature scaling is a common approach that involves scaling the output logits using a single scalar parameter T called *temperature*. This parameter is tuned to minimize the negative log-likelihood (also called cross-entropy) on a hold-out validation set. The newly calibrated probabilities are expressed as $\mathbf{p}_i = \sigma(\mathbf{z}_i/T)$.

Vector scaling and **Matrix scaling** involve transforming the logits using a linear transformation with a matrix $\mathbf{W}$ and a bias vector $\mathbf{b}$: $\mathbf{p}_i = \sigma(\mathbf{W}\mathbf{z}_i + \mathbf{b})$. For vector scaling, the matrix is restricted to be diagonal, and the parameters $\mathbf{W}, \mathbf{b}$ are tuned to minimize the negative log-likelihood on a hold-out validation set.

However, all these techniques rely on a labeled validation set from the source domain, and do not account for the shift between the source and target distribution.

Calibrated Prediction with Covariate Shift (CPCS) [36] proposes to correct for covariate shift by combining adversarial feature alignment (as in DANN [18]), importance weighting using a logistic domain discriminator, and temperature scaling. First, domain-invariant features are learned through domain-adversarial training. Then, a logistic domain discriminator is trained and its output probabilities are used to compute the importance weight $w(\mathbf{x}_i)$ for each sample. Specifically, the weight is equal to the ratio between the probability of belonging to the target domain and the probability of belonging to the source domain, allowing for a *translation* from the source distribution to the target one. Finally, the optimal temperature is found by minimizing the weighted Brier score [62] (i.e., the mean squared error between outputs and one-hot labels) on a hold-out source validation set.

3 Proposed method

3.1 Overview

We propose the Calibrated Adaptive Teacher (CAT) framework for unsupervised domain adaptation, an extension of the Adaptive Teacher (AT) [54]. CAT aims to improve the quality of pseudo-labels generated by the teacher network in the target domain. The primary innovation of this architecture lies in introducing post-hoc calibration into the self-training process.

The architecture, summarized in Figure 1, comprises two networks: a teacher and a student network, sharing the same architecture but with different weights. In the student network, both source and target inputs first pass through a feature encoder. This encoder consists of a 1D-CNN followed by a 256-dimensional bottleneck, as detailed in [3]. Subsequently, source and target fault classes are predicted by a fully-connected (FC) linear layer with softmax activation. The source and target features are also fed into the gradient reversal layer (GRL) and domain classifier (DC) for domain-adversarial training. The weights of each component in the student network are then updated through gradient descent training, using the loss function detailed in the following paragraphs. On the teacher side, only target inputs go through a

Table 1: Comparison of self-training unsupervised domain adaptation methods applied to intelligent fault diagnosis.

Method	Backbone	Time	Frequency	Feature alignment	Self-training	Pseudo-label filtering	Auxiliary loss
PCG-CNN [45]	1D-CNN	✓		-	MT with Consistency loss	fixed threshold	class-balance loss
Wang *et al.* [48]	1D-CNN	✓		DAW	PL	adaptive threshold	triplet loss
DTL-IPLL [46]	1D-CNN	✓		MK-MMD	PL	adaptive threshold + "make-decision-twice"	-
CAT (Ours)	1D-CNN	✓	✓	DANN	MT with PL	adaptive threshold + calibration	-

Module	Layers	Parameters	Notation
1D-CNN Backbone	Conv1D, BatchNorm, ReLU	in=1, out=16, kernel=15	$\mathbf{W}_{\text{E}}$
	Conv1D, BatchNorm, ReLU	in=16, out=32, kernel=3	
	MaxPool1D	kernel=2, stride=2	
	Conv1D, BatchNorm, ReLU	in=32, out=64, kernel=3	
	Conv1D, BatchNorm, ReLU	in=64, out=128, kernel=3	
	AdaptiveMaxPool1D	out=128×4	
	FC, ReLU	in=128×4, out=256	
	Dropout	p=0.5	
Bottleneck	FC, ReLU	in=256, out=256	
	Dropout	p=0.5	
Classification head	FC, Softmax	in=256, out=13	$\mathbf{W}_{\text{C}}$
Domain Classifier	FC, ReLU	in=256, out=1024	$\mathbf{W}_{\text{DC}}$
	Dropout	p=0.5	
	FC, ReLU	in=1024, out=1024	
	Dropout	p=0.5	
	FC, Sigmoid	in=1024, out=1	

Table 2: Parameters of the CAT architecture used in this study.

feature encoder and a linear classification head. Teacher predictions are then used to supervise the student through pseudo-labeling. Before selecting the pseudo-labels based on confidence, we introduce post-hoc calibration to calibrate the teacher predictions, which is the primary novelty in this architecture. Essentially, this calibration transforms the target logits (i.e., the outputs before the softmax) to obtain better-calibrated probabilities after applying the softmax. We then select the most confident predictions as pseudo-labels, using a class-wise adaptive threshold instead of the fixed threshold used in [54]. These pseudo-labels serve as supervision for the student network to train on target samples. The teacher weights are frozen and updated through EMA of the student weights between each training iteration, as presented on Figure 1.

We compare existing UDA approaches for IFD based on self-training with pseudo-labels in Table 1. To the best of our knowledge, none of these works has investigated the aspect of model calibration. The details of each layer in the architecture are provided in Table 2. Following this overview of our proposed approach, we introduce the key components in more detail.

3.2 Calibrated self-training

A model is considered well-calibrated if its confidence scores align with the accuracy of predictions. Since our objective is to increase the accuracy of selected pseudo-labels, and confidence serves as a proxy for accuracy, we aim for well-calibrated target outputs. Therefore, we propose calibrating the teacher network's outputs before selecting confident pseudo-labels for training. To achieve this calibration, we leverage a post-hoc calibration technique. Different post-hoc calibration techniques are available for multi-class classification, with differences in effectiveness and amount of parameters. In this study, we compare four previously introduced post-hoc calibration techniques: temperature scaling, vector scaling, matrix scaling, and calibrated predictions with covariate shift (CPCS) [36]. All these techniques rely on a labeled hold-out set from the source domain to learn a transformation of the target logits. Temperature scaling, with a single scalar parameter, was identified to be the most effective method in the study by Guo *et al.* [33]. Additionally, we evaluate vector and matrix scaling, which adjust each class differently, requiring $2K$ and $K^2 + K$ parameters, respectively. The first three techniques do not account for distribution shifts. In the context of a domain shift, we also evaluate CPCS, which addresses covariate shift by applying importance weighting with a logistic domain discriminator on domain-invariant features. These features are obtained through the domain classifier in our approach.

Definition (Calibrated self-training)**.** Let $\mathbf{x}$ be an unlabeled input, and $\mathbf{z}$ be the logits obtained from the teacher network before the softmax activation σ. The calibrated teacher predictions are defined as:

$$\mathbf{p}^{\text{cal}}_{\text{teacher}}(\mathbf{x}) = \sigma(f(\mathbf{z})) \tag{5}$$

where $f : \mathbb{R}^K \to \mathbb{R}^K$ is a calibration function operating on the logits.

We propose four variants of CAT, each incorporating different calibration techniques.

CAT - TempScaling The calibration function is as follows:

$$f : \mathbf{z} \mapsto \mathbf{z}/T^\star \text{ where } T^\star = \underset{T\in\mathbb{R}}{\arg\min} - \frac{1}{|\mathbf{X}^{\text{S}}_{\text{test}}|} \sum_{(\mathbf{x},y)} \sum_{k=1}^{K} \mathbb{1}(y = k) \cdot \log \sigma(\mathbf{z}/T)[k] \tag{6}$$

CAT - VectorScaling The calibration function is defined as follows:

$$f : \mathbf{z} \mapsto \mathbf{W}^\star\mathbf{z} + \mathbf{b}^\star \text{ where } \mathbf{W}^\star, \mathbf{b}^\star = \underset{(\mathbf{W},\mathbf{b})\in\text{diag}(K)\times\mathbb{R}^K}{\arg\min} - \frac{1}{|\mathbf{X}^{\text{S}}_{\text{test}}|} \sum_{(\mathbf{x},y)} \sum_{k=1}^{K} \mathbb{1}(y = k) \cdot \log \sigma(\mathbf{W}\mathbf{z} + \mathbf{b})[k] \tag{7}$$

CAT - MatrixScaling The calibration function is defined as follows:

$$f : \mathbf{z} \mapsto \mathbf{W}^\star\mathbf{z} + \mathbf{b}^\star \text{ where } \mathbf{W}^\star, \mathbf{b}^\star = \underset{(\mathbf{W},\mathbf{b})\in\mathbb{R}^{K\times K}\times\mathbb{R}^K}{\arg\min} - \frac{1}{|\mathbf{X}^{\text{S}}_{\text{test}}|} \sum_{(\mathbf{x},y)} \sum_{k=1}^{K} \mathbb{1}(y = k) \cdot \log \sigma(\mathbf{W}\mathbf{z} + \mathbf{b})[k] \tag{8}$$

CAT - CPCS (Calibrated Predictions with Covariate Shift) The calibration function is defined as follows:

$$f : \mathbf{z} \mapsto \mathbf{z}/T^\star \text{ where } T^\star = \underset{T\in\mathbb{R}}{\arg\min} - \frac{1}{|\mathbf{X}^{\text{S}}_{\text{test}}|} \sum_{(\mathbf{x},y)} w(\mathbf{x}) \sum_{k=1}^{K} \left(\mathbb{1}(y = k) - \sigma(\mathbf{z}/T)[k]\right)^2 \tag{9}$$

where the first summations are over the source test samples and labels $\mathbf{X}^{\text{S}}_{\text{test}} \times \mathbf{Y}^{\text{S}}_{\text{test}}$. In the case of CPCS, the importance weights $w(\mathbf{x})$ are derived from the source and target training samples, as explained in Section 2. All optimization problems for finding the optimal calibration parameters are convex and solved using the `optimize.fmin` function from `scipy`.

3.3 Adaptive confidence threshold

Curriculum pseudo-labeling methods dynamically adjust the confidence threshold for each class during training, based on the accuracy of each class. We adopt the method introduced in [25]. At training iteration t, the dynamic threshold for class k is defined as:

$$\mathcal{T}_t(k) = a_t(k) \cdot \tau \tag{10}$$

where $a_t(k)$ represents the accuracy, and τ is a fixed threshold value. As proposed in [25], the accuracy can be substituted with the *learning effect* of the class, which is reflected by the number of high-confidence predictions for this class:

$$\sigma_t(k) = \sum_{\mathbf{x}\in\mathbf{X}^{\text{T}}_{\text{train}}} \mathbb{1}(\max \mathbf{p}_{\text{teacher}}(\mathbf{x}) \geq \tau) \cdot \mathbb{1}(\arg\max_y \mathbf{p}_{\text{teacher}}(\mathbf{x})[y] = k) \tag{11}$$

Subsequently, this quantity is scaled, undergoes a non-linear mapping $\mathcal{M}$, and is ultimately used to define the dynamic threshold as follows:

$$\beta_t(k) = \frac{\sigma_t(k)}{\max_k \sigma_t(k)} \tag{12}$$

$$\mathcal{M}(x) = \frac{x}{2 - x} \tag{13}$$

$$\mathcal{T}_t(k) = \mathcal{M}(\beta_t(k)) \cdot \tau \tag{14}$$

At training iteration t, we ultimately define the set of selected target pseudo-labels:

$$\hat{\mathbf{X}}^{\mathrm{T}}_{\text{train}} = \{\mathbf{x}\ ;\ \mathbf{x} \in \mathbf{X}^{\mathrm{T}}_{\text{train}}, \max \mathbf{p}_{\text{teacher}}(\mathbf{x}) \geq \mathcal{T}_t(\arg\max_y \mathbf{p}_{\text{teacher}}(\mathbf{x})[y])\} \tag{15}$$

$$\hat{\mathbf{Y}}^{\mathrm{T}}_{\text{train}} = \{\arg\max_y \mathbf{p}_{\text{teacher}}(\mathbf{x})[y]\ ;\ \mathbf{x} \in \mathbf{X}^{\mathrm{T}}_{\text{train}}, \max \mathbf{p}_{\text{teacher}}(\mathbf{x}) \geq \mathcal{T}_t(\arg\max_y \mathbf{p}_{\text{teacher}}(\mathbf{x})[y])\} \tag{16}$$

In our CAT method, the teacher probabilities $\mathbf{p}_{\text{teacher}}(\mathbf{x})$ are replaced with the calibrated teacher probabilities $\mathbf{p}^{\text{cal}}_{\text{teacher}}(\mathbf{x})$.

3.4 Loss function and training procedure

3.4.1 Student training

We denote the parameters of the student network as $\boldsymbol{\theta} = \{\mathbf{W}_{\mathrm{E}}, \mathbf{W}_{\mathrm{C}}\}$, where $\mathbf{W}_{\mathrm{E}}$ and $\mathbf{W}_{\mathrm{C}}$represent the weights of the student encoder and classification head, respectively. The weights of the discriminator are denoted as $\mathbf{W}_{\mathrm{DC}}$. Instead of the standard DANN [18], we adopt the enhanced approach of Smooth Domain-Adversarial Training (SDAT) [63]. This involves using the Sharpness Aware Minimization (SAM) optimizer [64] on the task loss (i.e., supervised source loss) and incorporating the Minimum Class Confusion (MCC) loss [65], which stands as a current state-of-the-art method for domain adaptation in computer vision tasks. The MCC loss serves as a non-adversarial regularization term designed to minimize pairwise class confusion in the target domain.

The loss function of CAT, denoted $\mathcal{L}_{\text{CAT}}$, comprises four terms: a supervised source loss $\mathcal{L}_{\mathrm{C}}$, a target pseudo-labeling loss $\mathcal{L}_{\text{PL}}$, the domain classifier term $\mathcal{L}_{\text{DC}}$, and the MCC loss $\mathcal{L}_{\text{MCC}}$. The supervised loss is calculated as the cross-entropy between source predictions and labels:

$$\mathcal{L}_{\mathrm{C}}(\boldsymbol{\theta}; \mathbf{X}^{\mathrm{S}}_{\text{train}}, \mathbf{Y}^{\mathrm{S}}_{\text{train}}) = -\frac{1}{|\mathbf{X}^{\mathrm{S}}_{\text{train}}|} \sum_{(\mathbf{x},y)} \sum_{k=1}^{K} \mathbb{1}(y = k) \cdot \log \mathbf{p}(\mathbf{x})[k] \tag{17}$$

where the first summation is over the source training samples and labels $\mathbf{X}^{\mathrm{S}}_{\text{train}} \times \mathbf{Y}^{\mathrm{S}}_{\text{train}}$. The pseudo-labeling loss is then calculated as the cross-entropy between predictions and the pseudo-labels:

$$\mathcal{L}_{\text{PL}}(\boldsymbol{\theta}; \hat{\mathbf{X}}^{\mathrm{T}}_{\text{train}}, \hat{\mathbf{Y}}^{\mathrm{T}}_{\text{train}}) = -\frac{1}{|\hat{\mathbf{X}}^{\mathrm{T}}_{\text{train}}|} \sum_{(\mathbf{x},y)} \sum_{k=1}^{K} \mathbb{1}(y = k) \cdot \log \mathbf{p}(\mathbf{x})[k] \tag{18}$$

where the first summation is over the pseudo-labels $\hat{\mathbf{X}}^{\mathrm{T}}_{\text{train}} \times \hat{\mathbf{Y}}^{\mathrm{T}}_{\text{train}}$. The domain classifier loss is then expressed as a binary cross-entropy between the domain classifier predictions and domain labels, which is set to 1 for the source and 0 for the target training samples:

$$\mathcal{L}_{\text{DC}}(\mathbf{W}_{\mathrm{E}}, \mathbf{W}_{\text{DC}}; \mathbf{X}^{\mathrm{S}}_{\text{train}}, \mathbf{X}^{\mathrm{T}}_{\text{train}}) = -\frac{1}{|\mathbf{X}^{\mathrm{S}}_{\text{train}}|} \sum_{\mathbf{x} \in \mathbf{X}^{\mathrm{S}}_{\text{train}}} \log \mathbf{p}_{\text{DC}}(\mathbf{x}) - \frac{1}{|\mathbf{X}^{\mathrm{T}}_{\text{train}}|} \sum_{\mathbf{x} \in \mathbf{X}^{\mathrm{T}}_{\text{train}}} \log\left(1 - \mathbf{p}_{\text{DC}}(\mathbf{x})\right) \tag{19}$$

Finally, the total loss is an equally-weighted sum of the individual loss terms:

$$\mathcal{L}_{\text{CAT}}(\boldsymbol{\theta}, \mathbf{W}_{\text{DC}}; \mathbf{X}^{\mathrm{S}}_{\text{train}}, \mathbf{Y}^{\mathrm{S}}_{\text{train}}, \hat{\mathbf{X}}^{\mathrm{T}}_{\text{train}}, \hat{\mathbf{Y}}^{\mathrm{T}}_{\text{train}}) = \mathcal{L}_{\mathrm{C}} - \mathcal{L}_{\text{DC}} + \mathcal{L}_{\text{PL}} + \mathcal{L}_{\text{MCC}}, \tag{20}$$

omitting the arguments of each loss term for brevity. Source and target cross-entropies are given equal weights, and [65] found that a weight of 1 for the MCC loss worked across all their experiments. For the domain-adversarial training, we adopt the same strategy as [18] only used in [3], progressively increasing the GRL coefficient from 0 to 1 following the formula $\frac{2}{1+\exp(-10p)}$, where p increases linearly from 0 to 1 during training. The total loss is minimized with respect to the student weights, while the domain classifier loss is minimized w.r.t. the discriminator weights and maximized w.r.t. the encoder weights in an adversarial way via the gradient reversal layer. Thus, the overall objective is expressed as follows:

$$\min_{\boldsymbol{\theta}} \max_{\mathbf{W}_{\text{DC}}} \mathcal{L}_{\text{CAT}}(\boldsymbol{\theta}, \mathbf{W}_{\text{DC}}; \mathbf{X}^{\mathrm{S}}_{\text{train}}, \mathbf{Y}^{\mathrm{S}}_{\text{train}}, \hat{\mathbf{X}}^{\mathrm{T}}_{\text{train}}, \hat{\mathbf{Y}}^{\mathrm{T}}_{\text{train}}) \tag{21}$$

3.4.2 Student updating

The teacher network parameters are initialized with the student weights at the beginning of self-training. Subsequently, they are updated between each training iteration by EMA of the student weights with an update rate α:

$$\boldsymbol{\theta}_{\text{teacher}} \leftarrow \alpha \cdot \boldsymbol{\theta}_{\text{teacher}} + (1-\alpha) \cdot \boldsymbol{\theta} \tag{22}$$

3.5 Training procedure of the entire pipeline

The CAT training procedure consists of three phases. The first phase involves a source-only training of the student network using only the supervised loss $\mathcal{L}_{\text{C}}$. In the second phase, the domain classifier loss is enabled after T_{DA} epochs for domain-adversarial training. The third phase, mutual teacher-student training, begins at T_{PL}, with $T_{\text{DA}} \leq T_{\text{PL}}$. A warm-up phase is necessary to ensure sufficient pseudo-label quality and to avoid compromising the training by fitting noise [29]. Lastly, the calibration is enabled later in the training at T_{cal}, with $T_{\text{PL}} \leq T_{\text{cal}}$.

During the mutual training phase, at the beginning of each given epoch t, we estimate the class class-wise adaptive threshold values $\mathcal{T}_t(k)$ following (14), as well as the calibration function following (6) in CAT-TempScaling, (7) in CAT-VectorScaling, (8) in CAT-MatrixScaling and (9) in CAT-CPCS, depending on the variant of CAT considered. These estimations involve the unlabeled target training set and the labeled source test set. At every training iteration, a batch of inputs and labels is sampled from the source training set, and an unlabeled batch of inputs is sampled from the target training set. We compute and calibrate the logits of the teacher network to obtain calibrated probabilities, which are subsequently filtered using the adaptive threshold following (15,16). We then minimize the objective (21) by taking a gradient descent step. Finally, the teacher weights are updated by EMA following (22).

The complete training procedure is detailed in Algorithm 1.

4 Experiments

In this section, we discuss the data and transfer learning tasks, and provide details on the experimental settings and hyperparameters.

4.1 Case study

Experiments are conducted on the bearing fault diagnostics Paderborn University (PU) dataset [66], which comprises challenging transfer learning tasks across various operating conditions. The dataset comprises motor current signals of an electromechanical drive system, allowing for bearing diagnostics without the need for additional acceleration sensors for vibration analysis. The domain adaptation tasks involve adapting between four different operating conditions – rotational speed, load torque and radial force – described in Table 3.

We adopt the same setting as [3] for fair comparison. The classification problem has 13 classes and consists in classifying different combination of fault types and severities represented by different bearing codes, described in Table 4.

4.2 Training parameters

We train the model for a total of $T_{\text{total}} = 300$ epochs with a batch size of 64, using the Adam optimizer with a learning rate of 0.001, $\beta_1 = 0.9$, $\beta_1 = 0.999$ and a ℓ_2 weight decay of 10^{-5}. The learning rate is reduced by a factor 10 at epochs 150 and 250. The domain-adversarial loss is introduced at epoch $T_{\text{DA}} = 50$. Self-training starts at epoch $T_{\text{PL}} = 50$ for PU time-domain, and at epoch $T_{\text{DA}} = 100$ for PU frequency-domain. In both cases, we introduce the calibration from epoch $T_{\text{cal}} = 150$. The teacher EMA update rate is set to 0.999. The fixed threshold value in the adaptive threshold is $\tau = 0.9$. No weak-strong data augmentations were used. The train-test data splitting follows [3] with 80% of total samples for training and 20% for testing.

5 Results

In this section, we present the results of experiments on the PU dataset. First, we demonstrate the impact of our proposed calibration method on the quality of pseudo-labels and model performance in Section 5.1. Following this, Section 5.2 and Section 5.3 present a quantitative benchmark analysis comparing different UDA methods in terms of performance and calibration. We conduct ablation studies in Section 5.4.

Algorithm 1: Calibrated Adaptive Teacher (CAT) training procedure.

Data: $\mathbf{X}^{\mathrm{S}}_{\text{train}}, \mathbf{Y}^{\mathrm{S}}_{\text{train}}, \mathbf{X}^{\mathrm{S}}_{\text{test}}, \mathbf{Y}^{\mathrm{S}}_{\text{test}}, \mathbf{X}^{\mathrm{T}}_{\text{train}}$
Result: $\boldsymbol{\theta}, \boldsymbol{\theta}_{\text{teacher}}$

```
/* Phase 1: Source-only training */
```

for $epoch = 0$ **to** T_{DA} **do**
  for $iter = 0$ **to** $iterations$ **do**
    Sample source batch $\mathbf{x}^{\mathrm{S}}_{\text{train}}, \mathbf{y}^{\mathrm{S}}_{\text{train}}$
    Train on objective $\min_{\boldsymbol{\theta}} \mathcal{L}_{\mathrm{C}}(\boldsymbol{\theta}; \mathbf{x}^{\mathrm{S}}_{\text{train}}, \mathbf{y}^{\mathrm{S}}_{\text{train}})$
  end
end

```
/* Phase 2: Domain-adversarial training */
```

for $epoch = T_{DA}$ **to** T_{PL} **do**
  for $iter = 0$ **to** $iterations$ **do**
    Sample source and target batches $\mathbf{x}^{\mathrm{S}}_{\text{train}}, \mathbf{y}^{\mathrm{S}}_{\text{train}}, \mathbf{x}^{\mathrm{T}}_{\text{train}}$
    Train on objective $\min_{\boldsymbol{\theta}} \max_{\mathbf{W}_{\mathrm{DC}}} \mathcal{L}_{\mathrm{C}}(\boldsymbol{\theta}; \mathbf{x}^{\mathrm{S}}_{\text{train}}, \mathbf{y}^{\mathrm{S}}_{\text{train}}) - \mathcal{L}_{\mathrm{DC}}(\mathbf{W}_{\mathrm{E}}, \mathbf{W}_{\mathrm{DC}}; \mathbf{x}^{\mathrm{S}}_{\text{train}}, \mathbf{x}^{\mathrm{T}}_{\text{train}})$
  end
end

```
/* Phase 3: Mutual teacher-student training */
```

$\boldsymbol{\theta}_{\text{teacher}} \leftarrow \boldsymbol{\theta}$
for $epoch = T_{PL}$ **to** T_{total} **do**
  Estimate class-wise adaptive thresholds $\mathcal{T}_{epoch}(k)$ following (14)
  if $epoch \leq T_{cal}$ **then**
    Estimate calibration function following (6,7,8,9)
  end
  for $iter = 0$ **to** $iterations$ **do**
    Sample source and target batches $\mathbf{x}^{\mathrm{S}}_{\text{train}}, \mathbf{y}^{\mathrm{S}}_{\text{train}}, \mathbf{x}^{\mathrm{T}}_{\text{train}}$
    Predict target logits with teacher
    if $epoch \leq T_{cal}$ **then**
      Calibrate probabilities using calibration function
    end
    Generate pseudo-labels $\hat{\mathbf{x}}^{\mathrm{T}}_{\text{train}}, \hat{\mathbf{y}}^{\mathrm{T}}_{\text{train}}$ using adaptive threshold following (15,16)
    Train on objective $\min_{\boldsymbol{\theta}} \max_{\mathbf{W}_{\mathrm{DC}}} \mathcal{L}_{\mathrm{CAT}}(\boldsymbol{\theta}, \mathbf{W}_{\mathrm{DC}}; \mathbf{x}^{\mathrm{S}}_{\text{train}}, \mathbf{y}^{\mathrm{S}}_{\text{train}}, \hat{\mathbf{x}}^{\mathrm{T}}_{\text{train}}, \hat{\mathbf{y}}^{\mathrm{T}}_{\text{train}})$ following (21)
    Update teacher by EMA $\boldsymbol{\theta}_{\text{teacher}} \leftarrow \alpha \cdot \boldsymbol{\theta}_{\text{teacher}} + (1 - \alpha) \cdot \boldsymbol{\theta}$
  end
end

Table 3: Domains for the Paderborn University (PU) dataset.

Domain	Rotational speed	Load torque	Radial force
0	1500 rpm	0.7 Nm	1000 N
1	900 rpm	0.7 Nm	1000 N
2	1500 rpm	0.1 Nm	1000 N
3	1500 rpm	0.7 Nm	400 N

Table 4: Classification task for the Paderborn University (PU) dataset.

Class	Bearing code	Damage	Element	Combination	Characteristic
0	KA04	fatigue: pitting	OR	S	single point
1	KA15	plastic deform: indentations	OR	S	single point
2	KA16	fatigue: pitting	OR	R	single point
3	KA22	fatigue: pitting	OR	S	single point
4	KA30	plastic deform: indentations	OR	R	distributed
5	KB23	fatigue: pitting	IR(+OR)	M	single point
6	KB24	fatigue: pitting	IR(+OR)	M	distributed
7	KB27	plastic deform: indentations	OR+IR	M	distributed
8	KI14	fatigue: pitting	IR	M	single point
9	KI16	fatigue: pitting	IR	S	single point
10	KI17	fatigue: pitting	IR	R	single point
11	KI18	fatigue: pitting	IR	S	single point
12	KI21	fatigue: pitting	IR	S	single point

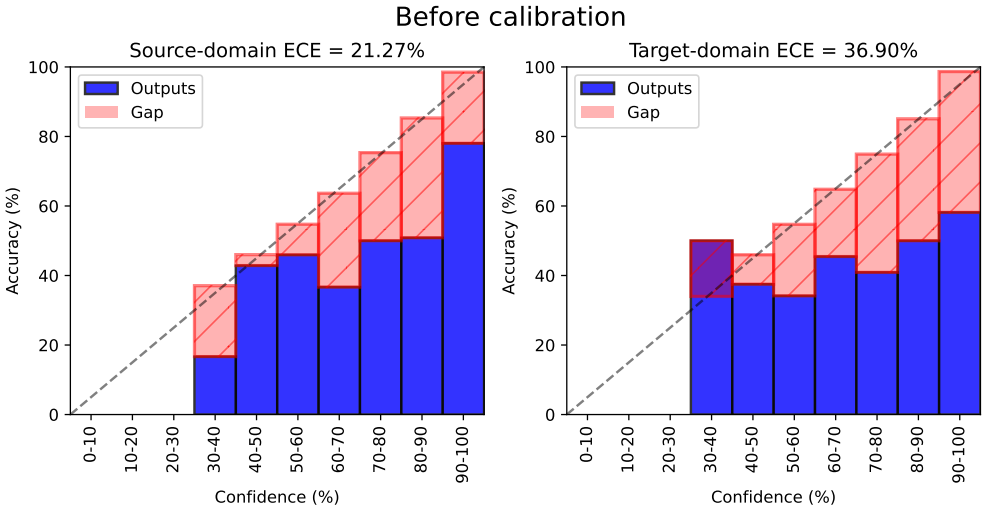

Figure 2: Example of reliability diagram before applying calibration (here, AT on the $0 \rightarrow 1$ task in time domain). The model has higher expected calibration error (ECE) on the target domain than on the source domain.

5.1 Calibration and quality of pseudo-labels

We begin by illustrating the motivation behind our approach, which is to address the issue of model calibration in the target domain, aiming to increase the accuracy of pseudo-labels.

In Figure 2, we present the reliability diagrams of the teacher predictions of a trained AT model on the source and target test sets. Blue bars under the diagonal represent over-confident predictions and vice-versa. The red area visualizes the gap between actual and ideal calibration. The initial observation is that the model is overconfident in both domains, but the expected calibration error (ECE) is even higher in the target domain (36.90%) than in the source domain (21.27%).

We present the same reliability diagrams after applying the temperature scaling (i.e., CAT-TempScaling) in Figure 3. Calibration drastically reduces the calibration error on the source domain to 5.41%, as expected, since the temperature was tuned on the source test set. However, it also significantly reduces the ECE on the target domain (down to 10.56%), even though temperature scaling does not account for domain shift. Thanks to feature alignment, the source and target distributions are similar enough to allow for a transfer of temperature scaling to the target data. Resulting reliability diagrams for vector and matrix scaling are shown and discussed in Appendix B.

As a consequence, we can expect the quality of the selected pseudo-labels to improve, as the confidence more closely matches the true accuracy, and we reduce the number of overconfident wrong target predictions. Figure 4 displays the evolution of target pseudo-label accuracy during training for the transfer task $0 \rightarrow 1$, comparing AT+MCC+SDAT

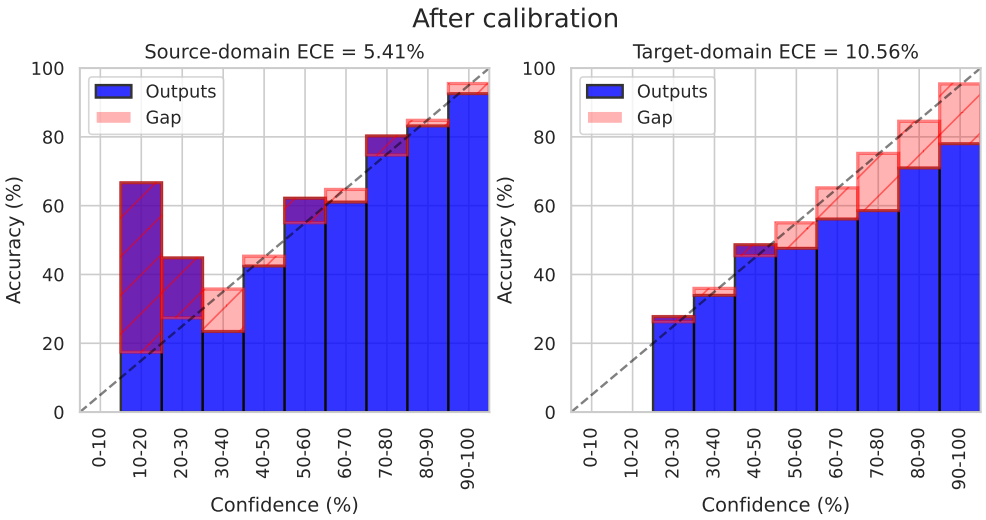

Figure 3: Example of reliability diagram after applying Temperature scaling (here, CAT on the $0 \rightarrow 1$ task in time domain). Even though temperature scaling is based on the source validation set, ECE is also drastically reduced on the target domain, owing to well-aligned features.

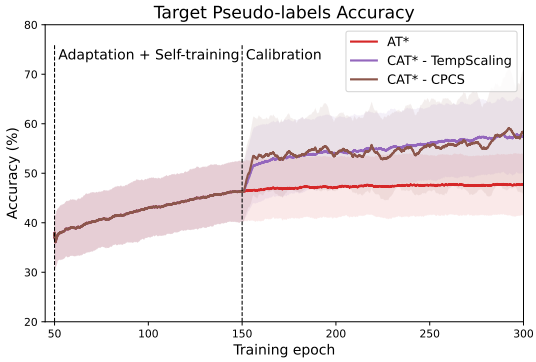

Figure 4: Evolution of target pseudo-labels accuracy produced by the teacher network during training for different methods. A boost in accuracy is observed after introduction of the calibration in our proposed CAT.

(denoted by AT*) and our proposed methods CAT*-TempScaling and CAT*-CPCS. At the epoch where calibration is introduced, we observe an absolute increase in pseudo-label accuracy of around 10%, which is maintained during the rest of the training. At the last iteration, pseudo-label accuracy reaches 47.64% for AT*, and 57.37% and 58.45% for CAT*-TempScaling and CAT*-CPCS, respectively.

In addition, Figure 5 illustrates the evolution of target test accuracy and ECE during training for different methods. Specifically, we compare the source-only model, DANN, DANN+MCC+SDAT (denoted as DANN*), AT+MCC+SDAT (denoted as AT*) and our proposed methods CAT*-TempScaling and CAT*-CPCS. Domain adaptation and self-training both start at $T_{\text{DA}} = T_{\text{PL}} = 50$ epochs, and calibration is enabled at $T_{\text{cal}} = 150$ epochs. All domain adaptation methods drastically improve the performance compared to the source-only model. AT significantly improves over the DANN baseline, but still exhibits a high ECE. After introducing calibration, the ECE drops significantly (see Figure 5, right), and the increased pseudo-label accuracy also translates into an improvement in accuracy on the target validation set (see Figure 5, left).

5.2 Comparative analysis of performance

In this section, we conduct a comparative analysis on the 12 transfer tasks of the PU bearing fault diagnosis benchmark, considering both time-domain and frequency-domain (FFT) inputs. In most related works, only time-domain inputs are considered (see Table 1). The compared methods include the model trained on the source (source-only), DANN,

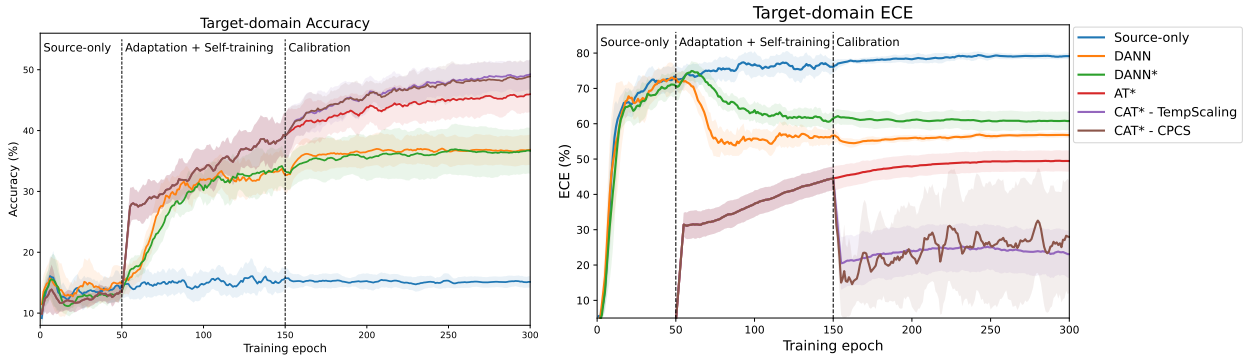

Figure 5: Evolution of target accuracy (left) and ECE (right) during training (here, on the $0 \rightarrow 1$ task in time domain). AT significantly improves over the DANN baseline. In addition, our proposed CAT effectively reduces calibration error, leading to an improved accuracy.

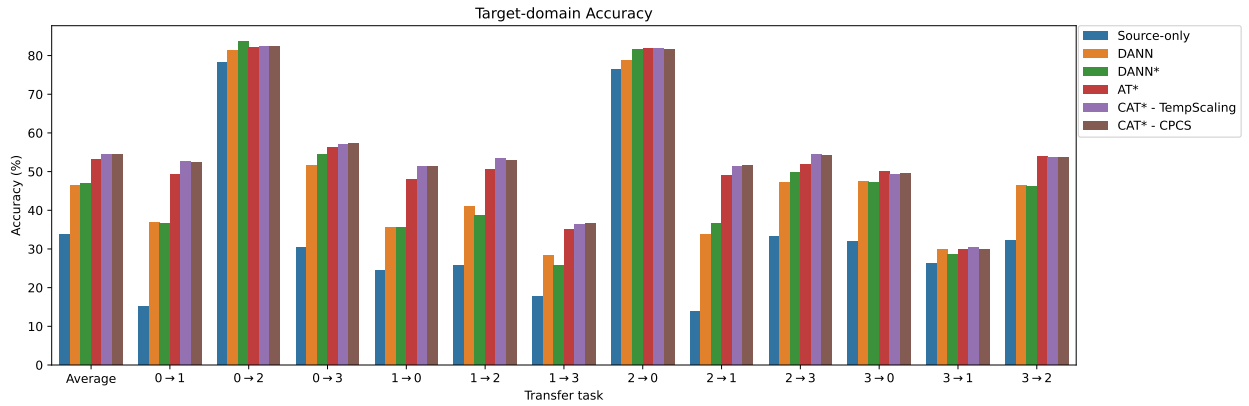

Figure 6: Comparison of target accuracy for different methods on the PU transfer tasks with time-domain input.

which is the best-performing domain adaptation method overall in the survey [3] and represents our main baseline, and DANN+MCC+SDAT (denoted as DANN*, where the asterisk indicates that the model integrates the MCC loss and SDAT [63]). We also evaluate AT*, our adaptation of AT [54]. Finally, we assess our proposed calibrated self-training methods CAT* with four different post-hoc calibration techniques, namely CAT*-TempScaling, CAT*-CPCS, CAT*-VectorScaling and CAT*-MatrixScaling. In the case of teacher-student models, we always report the results of the teacher network throughout the paper.

We use the same parameters as [3] for the source-only and DANN training. We assess the performance at the last training iteration, as using the test labels for early stopping is unrealistic. Thus, we compare our results to the "Last-Mean" results of [3]. All our experiments are repeated five times with different random seeds. As a performance measure, we report the average accuracy per transfer task and the overall average accuracy. Additionally, we report the average rank, which is better suited for comparing multiple methods over multiple tasks of varying difficulties [67].

Results for the PU dataset in time domain are presented in Figure 6 and Table 5. The domain adaptation baseline DANN achieves an overall accuracy of 46.53% across all tasks, consistent with the results reported by [3], and significantly higher than the source-only model (33.78%). It is worth noting that some transfer tasks are easy, with the source model already performing well ($0 \rightarrow 2$ and $2 \rightarrow 0$), while other tasks are challenging with accuracies below 50%. DANN* (DANN+MCC+SDAT) has a slightly higher average accuracy of 47.02%. The AT* method obtains a significantly higher average accuracy of 53.13%, outperforming DANN* on every task except the easiest one ($0 \rightarrow 2$). Overall, the best-performing methods are our proposed CAT*-TempScaling and CAT*-CPCS, with average accuracies of 54.50% and 54.42%, and average ranks of 2.28 and 2.40. The calibrated methods outperform the non-calibrated versions in 10 out of 12 tasks. Among the four calibration techniques, we observe that only TempScaling and CPCS are effective, whereas VectorScaling and MatrixScaling degrade the performance in most tasks.

The results for frequency-domain inputs are presented in Figure 7 and Table 6. The findings are consistent with those in time domain, and the methods exhibit similar average ranks. The source-only performance is higher than in the time

Table 5: Target-domain accuracy on the different PU transfer tasks with time-domain input (accuracy in %).

Method	$0 \to 1$	$0 \to 2$	$0 \to 3$	$1 \to 0$	$1 \to 2$	$1 \to 3$	$2 \to 0$	$2 \to 1$	$2 \to 3$	$3 \to 0$	$3 \to 1$	$3 \to 2$	Average	Average rank
Source-only†	14.02	76.33	30.02	23.57	24.18	16.09	76.73	14.71	31.23	32.16	25.27	32.39	33.06	-
DANN†	38.19	79.97	53.74	35.42	39.57	27.05	79.20	36.53	49.23	47.93	27.45	47.57	46.82	-
Source-only	15.15	78.23	30.29	24.33	25.71	17.73	76.41	13.87	33.34	31.92	26.32	32.12	33.78	7.90
DANN	36.96	81.22	51.56	35.55	40.89	28.35	78.77	33.83	47.29	47.56	29.94	46.41	46.53	5.49
DANN*	36.53	**83.54**	54.46	35.61	38.53	25.75	81.44	36.53	49.86	47.25	28.50	46.20	47.02	5.08
AT*	49.36	82.17	56.16	47.83	50.66	34.92	81.72	49.11	51.80	**50.08**	29.91	**53.86**	53.13	3.26
CAT* - TempScaling	**52.67**	82.44	57.00	**51.27**	**53.34**	36.34	81.78	51.44	**54.40**	49.22	30.37	53.74	**54.50**	**2.28**
CAT* - CPCS	52.42	82.29	**57.25**	51.24	52.76	**36.46**	81.69	**51.63**	54.25	49.40	29.88	53.77	54.42	**2.40**
CAT* - VectorScaling	34.51	82.08	50.95	43.66	45.53	34.10	**82.03**	40.18	48.35	47.99	**35.92**	46.75	49.34	4.15
CAT* - MatrixScaling	33.65	82.08	48.20	39.97	44.58	32.04	80.95	35.37	46.14	44.73	31.01	43.48	46.85	5.43

† = results from [3] (last/mean). * = with MCC + SDAT.

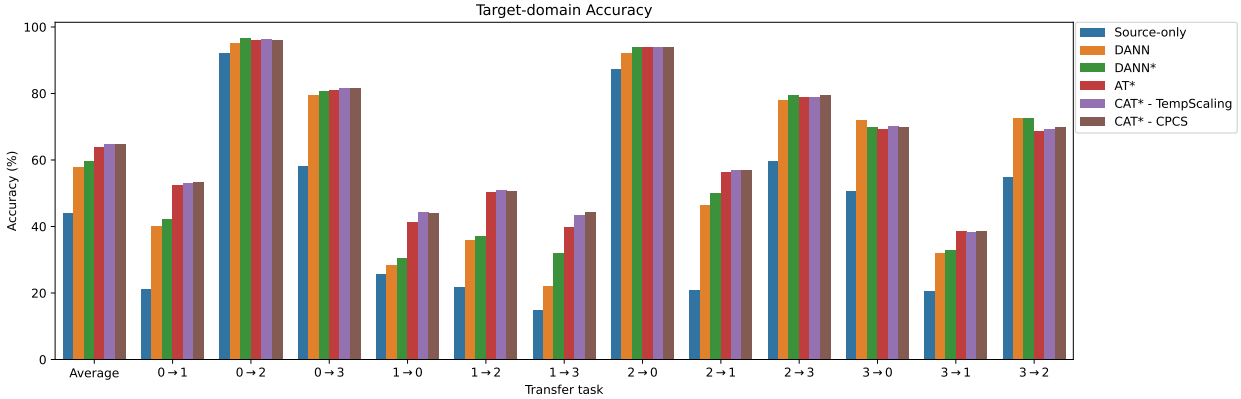

Figure 7: Comparison of target accuracy for different methods on the PU transfer tasks with frequency-domain input.

Table 6: Target-domain accuracy on the different PU transfer tasks with frequency-domain input (accuracy in %).

Method	$0 \to 1$	$0 \to 2$	$0 \to 3$	$1 \to 0$	$1 \to 2$	$1 \to 3$	$2 \to 0$	$2 \to 1$	$2 \to 3$	$3 \to 0$	$3 \to 1$	$3 \to 2$	Average	Average rank
Source-only†	20.96	90.87	57.14	25.13	24.14	13.75	86.40	20.55	57.18	52.58	20.90	53.64	43.60	-
DANN†	40.34	93.71	82.15	28.48	35.27	22.88	92.50	46.01	79.52	68.76	24.57	76.15	57.53	-
Source-only	21.13	92.12	58.34	25.68	21.92	14.92	87.47	20.83	59.76	50.81	20.71	54.75	44.04	7.98
DANN	40.09	95.27	79.58	28.45	35.88	22.15	92.07	46.44	78.03	**71.98**	32.09	72.61	57.89	5.76
DANN*	42.30	**96.58**	80.64	30.41	37.07	31.98	93.98	50.00	79.64	69.83	32.98	**72.73**	59.84	4.63
AT*	52.55	96.12	81.09	41.41	50.44	39.85	93.86	56.50	79.03	69.28	38.53	68.64	63.94	3.80
CAT* - TempScaling	52.98	96.27	81.57	**44.45**	**50.87**	43.36	93.89	**56.99**	79.06	70.11	38.22	69.34	64.76	**2.76**
CAT* - CPCS	**53.47**	96.18	**81.60**	43.96	50.60	**44.33**	93.89	56.93	**79.58**	70.05	**38.71**	69.77	**64.92**	**2.76**
CAT* - VectorScaling	50.92	96.40	81.24	43.53	48.40	41.97	**94.10**	55.18	78.61	69.25	37.55	69.50	63.89	3.64
CAT* - MatrixScaling	49.97	95.82	80.85	41.41	47.57	36.85	93.98	52.64	77.94	68.73	37.55	69.28	62.72	4.67

† = results from [3] (last/mean). * = with MCC + SDAT.

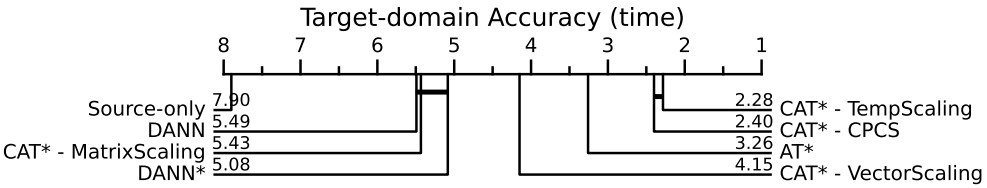

(a)

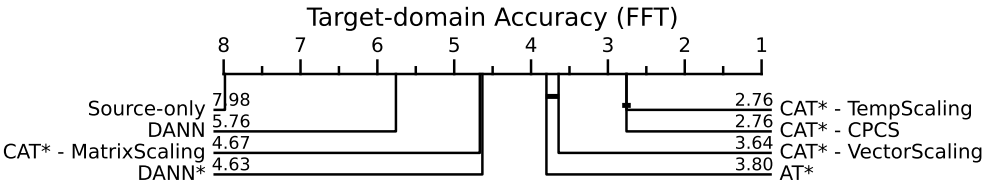

(b)

Figure 8: Critical difference diagrams of the performance of each method in terms of average rank of target accuracy on the PU transfer tasks in time-domain (a) and frequency-domain (b). Methods connected by a horizontal bar are statistically equivalent (using Wilcoxon-Holm post-hoc analysis at a 0.05 significance level).

domain, achieving 44.04% accuracy. The improvement of DANN* (59.84%) over DANN (57.89%) is more pronounced. Once again, the AT* method demonstrates a high average accuracy (63.94%) and significantly outperforms DANN* on all the challenging tasks, while showing comparable performance on the easier ones. As in the time domain, our proposed CAT*-TempScaling and CAT*-CPCS achieve the best performance, achieving 64.76% and 64.92% accuracy, with an equal average rank of 2.76 out of the 8 compared methods. CAT*-VectorScaling and CAT*-MatrixScaling, however, fail to improve upon AT*.

To assess the statistical significance of the differences between compared methods, we conducted a statistical post-hoc analysis using pairwise Wilcoxon signed-rank tests with Holm's step-down procedure at a significance level of 0.05 [67]. This procedure compares the sums of ranks across the 12 transfer tasks and 5 runs, testing against the null hypothesis stating that methods have equal performance. In Tables 5,6,7, the average ranks are reported in the rightmost column, with the rank of the best method and statistically equivalent methods in bold. As a result, our proposed CAT*-TempScaling and CAT*-CPCS have higher ranks than AT*, and this difference is significant in both the time and frequency domains. However, both calibration techniques are equivalent, indicating that the importance weighting in CPCS is not necessary in this case. The features are sufficiently well-aligned to make temperature scaling directly transferable and effective.

The result of the statistical tests are summarized in critical difference diagrams [67], shown in Figure 8. These diagrams visualize the average ranks of each method in terms of target accuracy, and connect statistically equivalent methods with a horizontal bar (i.e., when the null hypothesis could not be rejected at a significance level of 0.05). In both time and frequency domains, CAT*-TempScaling and CAT*-CPCS emerge as the top-performing methods with equivalent performance. The next-best methods, AT* and CAT*-VectorScaling, have significantly different ranks with time series inputs but not with FFT inputs. The CD-diagram[1] library was used to create these diagrams.

5.3 Comparative analysis of calibration error

In this section, we compare the calibration error in terms of expected calibration error (ECE), across different methods. The ECE of target-domain predictions is presented in Figure 9 and detailed in Table 7 for time-domain inputs, with frequency-domain results available in Appendix A. On average, both the source-only model and DANN exhibit very high ECE values, exceeding 50% on most tasks, particularly the challenging ones. While the Adaptive Teacher shows improved calibration, it still maintains a relatively high average ECE of 34.26%. CAT*-VectorScaling and CAT*-MatrixScaling fail to improve calibration in target domain on most tasks compared with AT*, aligning with their subpar accuracy performance. Finally, CAT*-TempScaling and CAT*-CPCS achieve the lowest calibration error, with average ECE values of 12.77% and 11.31%, and average ranks of 1.67 and 1.48, respectively.

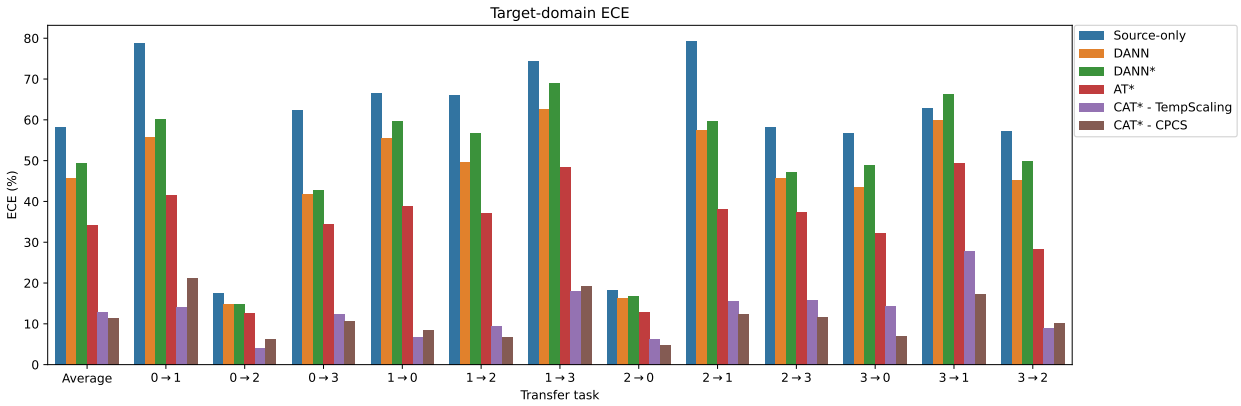

Figure 9: Comparison of target-domain expected calibration error (ECE) for different methods on the PU transfer tasks with time-domain input (lower is better).

Table 7: Target-domain expected calibration error (ECE) on the different PU transfer tasks with time-domain input (ECE in %, lower is better).

Method	$0 \to 1$	$0 \to 2$	$0 \to 3$	$1 \to 0$	$1 \to 2$	$1 \to 3$	$2 \to 0$	$2 \to 1$	$2 \to 3$	$3 \to 0$	$3 \to 1$	$3 \to 2$	Average	Average rank
Source-only	78.90	17.41	62.44	66.60	66.11	74.27	18.24	79.20	58.15	56.86	62.86	57.16	58.18	7.85
DANN	55.70	14.80	41.80	55.41	49.55	62.51	16.29	57.58	45.81	43.55	59.98	45.25	45.69	6.13
DANN*	60.17	14.81	42.89	59.57	56.73	68.97	16.86	59.73	47.24	48.83	66.33	49.83	49.33	6.88
AT*	41.51	12.60	34.33	38.96	37.04	48.46	12.90	38.07	37.27	32.34	49.30	28.29	34.26	4.15
CAT* - TempScaling	**14.16**	**3.95**	12.30	**6.64**	9.54	**18.10**	6.24	15.49	15.84	14.39	27.75	**8.87**	12.77	1.67
CAT* - CPCS	21.09	6.36	**10.76**	8.34	**6.77**	19.28	**4.89**	**12.44**	**11.63**	**6.94**	**17.19**	10.05	**11.31**	**1.48**
CAT* - VectorScaling	49.19	5.65	31.14	26.67	25.55	31.05	7.48	44.31	35.41	34.69	38.83	37.78	30.65	3.35
CAT* - MatrixScaling	54.38	8.03	36.62	27.25	25.97	32.55	11.29	48.81	41.30	39.78	47.16	42.60	34.64	4.48

* = with MCC + SDAT.

5.4 Ablation studies

In this section, we present the results of ablation studies, providing justification for the design choices in our proposed method and assessing the impact of each component. Initially, we compare the performance of the AT model using a fixed confidence threshold ($\tau = 0.9$) against an adaptive threshold, as introduced in Section 3. The results on the PU dataset in the time domain (see Table 8) indicate that, in most transfer tasks, particularly the most challenging ones, the adaptive threshold outperforms the fixed threshold in terms of target-domain teacher accuracy. The adaptive thresholding strategy achieves an average accuracy of 48.33%, whereas the fixed thresholding strategy averages 46.22% over all tasks.

In a second ablation study, we investigate the influence of incorporating the MCC loss [65] and the SDAT optimization technique [63] into the AT and CAT methods. We conducted experiments for AT, CAT-TempScaling and CAT-CPCS on the PU dataset in time domain, using different combinations of MCC and/or SDAT, as reported in Table 9. For each method, using MCC and SDAT together results in a substantial performance gain, consistent with findings by [63]. The average target-domain accuracy of the teacher network across all tasks is approximately 4% higher when using both MCC and SDAT compared to not using them.

6 Conclusion

In this paper, we tackled the challenge of model calibration for pseudo-labeling in the context of unsupervised domain adaptation. We proposed a novel method called Calibrated Adaptive Teacher (CAT), drawing inspiration from Mean Teacher, self-training with pseudo-labels, and feature alignment through domain-adversarial training. The primary innovation involves calibrating the predictions of the teacher network in the target domain throughout the self-training process. We explored four post-hoc calibration techniques, with temperature scaling and CPCS yielding the best results. Interestingly, both techniques performed similarly, despite the fact that the first one does not account for the domain shift. We believe this is due to the presence of already well-aligned features when calibration is introduced, enabling

[1] `https://github.com/hfawaz/cd-diagram`

Table 8: Comparison between fixed and adaptive confidence thresholds in Adaptive Teacher (AT). Results on PU dataset with time-domain input. Average teacher accuracy on target validation set over 5 runs (values in %).

Method	Threshold	$0 \to 1$	$0 \to 2$	$0 \to 3$	$1 \to 0$	$1 \to 2$	$1 \to 3$	$2 \to 0$	$2 \to 1$	$2 \to 3$	$3 \to 0$	$3 \to 1$	$3 \to 2$	Average
AT	fixed	33.44	**80.95**	49.53	40.98	39.39	23.00	**79.75**	36.60	44.21	**50.23**	**29.20**	47.33	46.22
AT	adaptive	**38.77**	80.89	**52.50**	**41.63**	**44.34**	**26.29**	78.86	**42.88**	**45.90**	49.03	28.99	**51.21**	**48.33**

Table 9: Ablation study on MCC and SDAT in Adaptive Teacher (AT) and our proposed Calibrated Adaptive Teacher (CAT) methods. Results on PU dataset with time-domain input. Average teacher accuracy on target validation set over 5 runs (values in %).

Method	MCC	SDAT	$0 \to 1$	$0 \to 2$	$0 \to 3$	$1 \to 0$	$1 \to 2$	$1 \to 3$	$2 \to 0$	$2 \to 1$	$2 \to 3$	$3 \to 0$	$3 \to 1$	$3 \to 2$	Average
AT			38.77	80.89	52.50	41.63	44.34	26.29	78.86	42.88	45.90	49.03	28.99	51.21	48.33
	✓		42.77	80.92	52.89	43.53	46.75	28.38	80.83	43.87	46.44	**51.34**	**32.73**	51.45	50.04
		✓	45.98	**82.32**	54.98	45.28	46.41	30.89	81.04	48.71	50.80	44.18	26.44	50.05	50.59
	✓	✓	**49.36**	82.17	**56.16**	**47.83**	**50.66**	**34.92**	**81.72**	**49.11**	**51.80**	50.08	29.91	**53.86**	**53.13**
CAT - TempScaling			44.58	81.40	53.95	47.04	46.99	27.87	78.92	44.82	48.14	49.59	28.99	52.18	50.28
	✓		46.56	81.34	55.16	48.91	50.14	32.44	81.17	46.38	48.35	**50.60**	**33.22**	53.07	52.28
		✓	49.14	82.41	56.58	47.50	49.92	32.47	81.01	50.00	52.34	44.70	23.19	50.14	51.62
	✓	✓	**52.67**	**82.44**	**57.00**	**51.27**	**53.34**	**36.34**	**81.78**	**51.44**	**54.40**	49.22	30.37	**53.74**	**54.50**
CAT - CPCS			43.90	81.53	53.86	46.18	46.44	27.35	79.17	44.29	48.53	49.62	30.15	52.40	50.28
	✓		46.87	81.34	54.89	48.82	50.38	32.95	81.17	46.78	48.59	**51.58**	**33.28**	52.89	52.46
		✓	49.82	**82.38**	57.19	47.37	49.65	30.98	81.01	51.23	52.68	45.19	23.40	49.71	51.72
	✓	✓	**52.42**	82.29	**57.25**	**51.24**	**52.76**	**36.46**	**81.69**	**51.63**	**54.25**	49.40	29.88	**53.77**	**54.42**

temperature scaling to transfer to the target domain. Experiments on intelligent fault diagnosis demonstrated that our method is able to improve calibration in the target domain, resulting in increased accuracy. On the Paderborn University bearing dataset, our method outperformed previous unsupervised domain adaptation approaches by a significant margin.

Our method is only effective whenever the model is badly calibrated in the target domain. The main limitation of our approach is that if target predictions are already well-calibrated, improvement cannot be expected. Additionally, we observed that our approach is more effective in tackling more challenging tasks, specifically when the baseline accuracy is relatively low.

The application of weak-strong data augmentations, as implemented in [54], requires further investigation in the context of intelligent fault diagnosis. The use of weak augmentations for the teacher network and strong augmentations for the student network is highly beneficial in computer vision applications. Exploring suitable augmentations for time series and spectrum data represents a promising direction for future research.

Acknowledgment

This study was supported by the Swiss National Science Foundation (grant number 200021_200461).

References

[1] Zhibin Zhao, Tianfu Li, Jingyao Wu, Chuang Sun, Shibin Wang, Ruqiang Yan, and Xuefeng Chen. Deep learning algorithms for rotating machinery intelligent diagnosis: An open source benchmark study. *ISA Transactions*, 107:224–255, December 2020.

[2] Yaguo Lei, Bin Yang, Xinwei Jiang, Feng Jia, Naipeng Li, and Asoke K. Nandi. Applications of machine learning to machine fault diagnosis: A review and roadmap. *Mechanical Systems and Signal Processing*, 138:106587, April 2020.

[3] Zhibin Zhao, Qiyang Zhang, Xiaolei Yu, Chuang Sun, Shibin Wang, Ruqiang Yan, and Xuefeng Chen. Applications of Unsupervised Deep Transfer Learning to Intelligent Fault Diagnosis: A Survey and Comparative Study. *IEEE Transactions on Instrumentation and Measurement*, 70:1–28, 2021. arXiv:1912.12528 [cs, eess].

[4] Weihua Li, Ruyi Huang, Jipu Li, Yixiao Liao, Zhuyun Chen, Guolin He, Ruqiang Yan, and Konstantinos Gryllias. A perspective survey on deep transfer learning for fault diagnosis in industrial scenarios: Theories, applications and challenges. *Mechanical Systems and Signal Processing*, 167:108487, March 2022.

[5] Ievgen Redko, Amaury Habrard, Emilie Morvant, Marc Sebban, and Younès Bennani. *Advances in Domain Adaptation Theory*. 2019.

[6] Qin Wang, Gabriel Michau, and Olga Fink. Domain Adaptive Transfer Learning for Fault Diagnosis. In *2019 Prognostics and System Health Management Conference (PHM-Paris)*, pages 279–285, May 2019. ISSN: 2166-5656.

[7] Min Huang, Jinghan Yin, Shumin Yan, and Pengcheng Xue. A fault diagnosis method of bearings based on deep transfer learning. *Simulation Modelling Practice and Theory*, 122:102659, January 2023.

[8] Gabriel Michau and Olga Fink. Domain Adaptation for One-Class Classification: Monitoring the Health of Critical Systems Under Limited Information. *International Journal of Prognostics and Health Management*, 10(4), 2019. Number: 4.

[9] Fei Shen, Reza Langari, and Ruqiang Yan. Transfer between multiple machine plants: A modified fast self-organizing feature map and two-order selective ensemble based fault diagnosis strategy. *Measurement*, 151:107155, February 2020.

[10] Jun Zhu, Nan Chen, and Changqing Shen. A New Multiple Source Domain Adaptation Fault Diagnosis Method Between Different Rotating Machines. *IEEE Transactions on Industrial Informatics*, 17(7):4788–4797, July 2021. Conference Name: IEEE Transactions on Industrial Informatics.

[11] Ismail Nejjar, Fabian Geissmann, Mengjie Zhao, Cees Taal, and Olga Fink. Domain adaptation via alignment of operation profile for Remaining Useful Lifetime prediction. *Reliability Engineering & System Safety*, 242:109718, February 2024.

[12] Bin Yang, Yaguo Lei, Feng Jia, and Saibo Xing. An intelligent fault diagnosis approach based on transfer learning from laboratory bearings to locomotive bearings. *Mechanical Systems and Signal Processing*, 122:692–706, May 2019.

[13] Qin Wang, Cees Taal, and Olga Fink. Integrating Expert Knowledge With Domain Adaptation for Unsupervised Fault Diagnosis. *IEEE Transactions on Instrumentation and Measurement*, 71:1–12, 2022. Conference Name: IEEE Transactions on Instrumentation and Measurement.

[14] Yunxia Lou, Anil Kumar, and Jiawei Xiang. Machinery Fault Diagnosis Based on Domain Adaptation to Bridge the Gap Between Simulation and Measured Signals. *IEEE Transactions on Instrumentation and Measurement*, 71:1–9, 2022. Conference Name: IEEE Transactions on Instrumentation and Measurement.

[15] Mingsheng Long, Yue Cao, Jianmin Wang, and Michael Jordan. Learning Transferable Features with Deep Adaptation Networks. In *Proceedings of the 32nd International Conference on Machine Learning*, pages 97–105. PMLR, June 2015. ISSN: 1938-7228.

[16] Kuniaki Saito, Kohei Watanabe, Yoshitaka Ushiku, and Tatsuya Harada. Maximum Classifier Discrepancy for Unsupervised Domain Adaptation. In *2018 IEEE/CVF Conference on Computer Vision and Pattern Recognition*, pages 3723–3732, Salt Lake City, UT, USA, June 2018. IEEE.

[17] Nicolas Courty, Rémi Flamary, Amaury Habrard, and Alain Rakotomamonjy. Joint distribution optimal transportation for domain adaptation. In *Advances in Neural Information Processing Systems*, 2017.

[18] Yaroslav Ganin, Evgeniya Ustinova, Hana Ajakan, Pascal Germain, Hugo Larochelle, François Laviolette, Mario March, and Victor Lempitsky. Domain-Adversarial Training of Neural Networks. *Journal of Machine Learning Research*, 17(59):1–35, 2016.

[19] Baorui Dai, Gaëtan Frusque, Tianfu Li, Qi Li, and Olga Fink. Smart filter aided domain adversarial neural network for fault diagnosis in noisy industrial scenarios. *Engineering Applications of Artificial Intelligence*, 126:107202, November 2023.

[20] Massih-Reza Amini, Vasilii Feofanov, Loic Pauletto, Lies Hadjadj, Emilie Devijver, and Yury Maximov. Self-Training: A Survey, September 2023. arXiv:2202.12040 [cs].

[21] Dong-Hyun Lee. Pseudo-Label : The Simple and Efficient Semi-Supervised Learning Method for Deep Neural Networks. *ICML 2013 Workshop : Challenges in Representation Learning (WREPL)*, July 2013.

[22] Avrim Blum and Tom Mitchell. Combining labeled and unlabeled data with co-training. In *Proceedings of the eleventh annual conference on Computational learning theory*, COLT' 98, pages 92–100, New York, NY, USA, July 1998. Association for Computing Machinery.

[23] Massih-Reza Amini and Patrick Gallinari. Semi-supervised logistic regression. In *Proceedings of the 15th European Conference on Artificial Intelligence*, ECAI'02, pages 390–394, NLD, July 2002. IOS Press.

[24] Yves Grandvalet and Yoshua Bengio. Semi-supervised Learning by Entropy Minimization. In *NIPS*, 2005.

[25] Bowen Zhang, Yidong Wang, Wenxin Hou, Hao Wu, Jindong Wang, Manabu Okumura, and Takahiro Shinozaki. FlexMatch: Boosting Semi-Supervised Learning with Curriculum Pseudo Labeling, January 2022. arXiv:2110.08263 [cs].

[26] Gokhan Tur, Dilek Hakkani-Tür, and Robert E. Schapire. Combining active and semi-supervised learning for spoken language understanding. *Speech Communication*, 45(2):171–186, February 2005.

[27] Weichen Zhang, Wanli Ouyang, Wen Li, and Dong Xu. Collaborative and Adversarial Network for Unsupervised Domain Adaptation. In *2018 IEEE/CVF Conference on Computer Vision and Pattern Recognition*, pages 3801–3809, June 2018. ISSN: 2575-7075.

[28] Yang Zou, Zhiding Yu, B. V. K. Vijaya Kumar, and Jinsong Wang. Domain Adaptation for Semantic Segmentation via Class-Balanced Self-Training, October 2018. arXiv:1810.07911 [cs].

[29] Ke Mei, Chuang Zhu, Jiaqi Zou, and Shanghang Zhang. Instance Adaptive Self-training for Unsupervised Domain Adaptation. In Andrea Vedaldi, Horst Bischof, Thomas Brox, and Jan-Michael Frahm, editors, *Computer Vision – ECCV 2020*, Lecture Notes in Computer Science, pages 415–430, Cham, 2020. Springer International Publishing.

[30] Zhedong Zheng and Yi Yang. Rectifying Pseudo Label Learning via Uncertainty Estimation for Domain Adaptive Semantic Segmentation. *International Journal of Computer Vision*, 129(4):1106–1120, April 2021.

[31] Geoffrey French, Michal Mackiewicz, and Mark Fisher. Self-ensembling for visual domain adaptation, September 2018. arXiv:1706.05208 [cs] version: 4.

[32] Ambroise Odonnat, Vasilii Feofanov, and Ievgen Redko. Leveraging Ensemble Diversity for Robust Self-Training in the Presence of Sample Selection Bias, October 2023. arXiv:2310.14814 [cs, stat].

[33] Chuan Guo, Geoff Pleiss, Yu Sun, and Kilian Q. Weinberger. On Calibration of Modern Neural Networks. In *Proceedings of the 34th International Conference on Machine Learning*, pages 1321–1330. PMLR, July 2017. ISSN: 2640-3498.

[34] Volodymyr Kuleshov, Nathan Fenner, and Stefano Ermon. Accurate Uncertainties for Deep Learning Using Calibrated Regression. In *Proceedings of the 35 th International Conference on Machine Learning*, volume 80, page 9, Stockholm, Sweden, 2018.

[35] Xiaogang Deng and Xianhui Jiang. On confidence computation and calibration of deep support vector data description. *Engineering Applications of Artificial Intelligence*, 125:106646, October 2023.

[36] Sangdon Park, Osbert Bastani, James Weimer, and Insup Lee. Calibrated Prediction with Covariate Shift via Unsupervised Domain Adaptation. In *Proceedings of the Twenty Third International Conference on Artificial Intelligence and Statistics*, pages 3219–3229. PMLR, June 2020. ISSN: 2640-3498.

[37] Muhammad Akhtar Munir, Muhammad Haris Khan, M Saquib Sarfraz, and Mohsen Ali. SSAL: Synergizing between Self-Training and Adversarial Learning for Domain Adaptive Object Detection. In *NeurIPS 2021*, page 13, 2021.

[38] Bo Zhang, Wei Li, Jie Hao, Xiao-Li Li, and Meng Zhang. Adversarial adaptive 1-D convolutional neural networks for bearing fault diagnosis under varying working condition, May 2018. arXiv:1805.00778 [cs, eess].

[39] D. She, N. Peng, M. Jia, and M. G. Pecht. Wasserstein distance based deep multi-feature adversarial transfer diagnosis approach under variable working conditions. *Journal of Instrumentation*, 15(06):P06002, June 2020.

[40] Feng Li, Tuojiang Tang, Baoping Tang, and Qiyuan He. Deep convolution domain-adversarial transfer learning for fault diagnosis of rolling bearings. *Measurement*, 169:108339, February 2021.

[41] Qunwang Yao, Quan Qian, Yi Qin, Liang Guo, and Fei Wu. Adversarial domain adaptation network with pseudo-siamese feature extractors for cross-bearing fault transfer diagnosis. *Engineering Applications of Artificial Intelligence*, 113:104932, August 2022.

[42] X. Wang, C. Shen, M. Xia, D. Wang, J. Zhu, and Z. Zhu. Multi-scale deep intra-class transfer learning for bearing fault diagnosis. *Reliability Engineering and System Safety*, 202, 2020.

[43] Yi Qin, Quan Qian, Zhengyi Wang, and Yongfang Mao. Adaptive manifold partial domain adaptation for fault transfer diagnosis of rotating machinery. *Engineering Applications of Artificial Intelligence*, 126:107082, November 2023.

[44] Sixiang Jia, Jinrui Wang, Baokun Han, Guowei Zhang, Xiaoyu Wang, and Jingtao He. A Novel Transfer Learning Method for Fault Diagnosis Using Maximum Classifier Discrepancy With Marginal Probability Distribution Adaptation. *IEEE Access*, 8:71475–71485, 2020. Conference Name: IEEE Access.

[45] Songsong Wu, Xiao-Yuan Jing, Qinghua Zhang, Fei Wu, Haifeng Zhao, and Yuning Dong. Prediction Consistency Guided Convolutional Neural Networks for Cross-Domain Bearing Fault Diagnosis. *IEEE Access*, 8:120089–120103, 2020. Conference Name: IEEE Access.

[46] Wenying Zhu, Boqiang Shi, and Zhipeng Feng. A Transfer Learning Method Using High-quality Pseudo Labels for Bearing Fault Diagnosis. *IEEE Transactions on Instrumentation and Measurement*, pages 1–1, 2022. Conference Name: IEEE Transactions on Instrumentation and Measurement.

[47] Yarin Gal and Zoubin Ghahramani. Dropout as a Bayesian Approximation: Representing Model Uncertainty in Deep Learning. In *Proceedings of The 33rd International Conference on Machine Learning*, pages 1050–1059. PMLR, June 2016. ISSN: 1938-7228.

[48] Jianyu Wang, Zhiguo Zeng, Heng Zhang, Anne Barros, and Qiang Miao. An hybrid domain adaptation diagnostic network guided by curriculum pseudo labels for electro-mechanical actuator. *Reliability Engineering & System Safety*, 228:108770, December 2022.

[49] Pengfei Chen, Rongzhen Zhao, Tianjing He, Kongyuan Wei, and Jianhui Yuan. Unsupervised structure subdomain adaptation based the Contrastive Cluster Center for bearing fault diagnosis. *Engineering Applications of Artificial Intelligence*, 122:106141, June 2023.

[50] Yang Hu, Piero Baraldi, Francesco Di Maio, and Enrico Zio. A Systematic Semi-Supervised Self-adaptable Fault Diagnostics approach in an evolving environment. *Mechanical Systems and Signal Processing*, 88:413–427, May 2017.

[51] Xinmin Tao, Chao Ren, Qing Li, Wenjie Guo, Rui Liu, Qing He, and Junrong Zou. Bearing defect diagnosis based on semi-supervised kernel Local Fisher Discriminant Analysis using pseudo labels. *ISA Transactions*, 110:394–412, April 2021.

[52] Xiaolong Zhang, Zuqiang Su, Xiaolin Hu, Yan Han, and Shuxian Wang. Semisupervised Momentum Prototype Network for Gearbox Fault Diagnosis Under Limited Labeled Samples. *IEEE Transactions on Industrial Informatics*, 18(9):6203–6213, September 2022. Conference Name: IEEE Transactions on Industrial Informatics.

[53] Jianyu Long, Yibin Chen, Zhe Yang, Yunwei Huang, and Chuan Li. A novel self-training semi-supervised deep learning approach for machinery fault diagnosis. *International Journal of Production Research*, pages 1–14, February 2022.

[54] Yu-Jhe Li, Xiaoliang Dai, Chih-Yao Ma, Yen-Cheng Liu, Kan Chen, Bichen Wu, Zijian He, Kris Kitani, and Peter Vajda. Cross-Domain Adaptive Teacher for Object Detection. In *2022 IEEE/CVF Conference on Computer Vision and Pattern Recognition (CVPR)*, page 10, 2022.

[55] Antti Tarvainen and Harri Valpola. Mean teachers are better role models: Weight-averaged consistency targets improve semi-supervised deep learning results, April 2018. arXiv:1703.01780 [cs, stat].

[56] Samuli Laine and Timo Aila. Temporal Ensembling for Semi-Supervised Learning, March 2017. arXiv:1610.02242 [cs].

[57] Yen-Cheng Liu, Chih-Yao Ma, Zijian He, Chia-Wen Kuo, Kan Chen, Peizhao Zhang, Bichen Wu, Zsolt Kira, and Peter Vajda. Unbiased Teacher for Semi-Supervised Object Detection, February 2021. arXiv:2102.09480 [cs].

[58] Alexandru Niculescu-Mizil and Rich Caruana. Predicting good probabilities with supervised learning. In *Proceedings of the 22nd international conference on Machine learning - ICML '05*, pages 625–632, Bonn, Germany, 2005. ACM Press.

[59] Mahdi Pakdaman Naeini, Gregory F. Cooper, and Milos Hauskrecht. Obtaining Well Calibrated Probabilities Using Bayesian Binning. *Proceedings of the ... AAAI Conference on Artificial Intelligence. AAAI Conference on Artificial Intelligence*, 2015:2901–2907, January 2015.

[60] Ramya Hebbalaguppe, Jatin Prakash, Neelabh Madan, and Chetan Arora. A Stitch in Time Saves Nine: A Train-Time Regularizing Loss for Improved Neural Network Calibration. In *2022 IEEE/CVF Conference on Computer Vision and Pattern Recognition (CVPR)*, pages 16060–16069, June 2022. ISSN: 2575-7075.

[61] Yaniv Ovadia, Emily Fertig, Jie Ren, Zachary Nado, D. Sculley, Sebastian Nowozin, Joshua V. Dillon, Balaji Lakshminarayanan, and Jasper Snoek. Can You Trust Your Model's Uncertainty? Evaluating Predictive Uncertainty Under Dataset Shift, December 2019. arXiv:1906.02530 [cs, stat].

[62] Glenn W. Brier. VERIFICATION OF FORECASTS EXPRESSED IN TERMS OF PROBABILITY. *Monthly Weather Review*, 78(1):1–3, January 1950. Publisher: American Meteorological Society Section: Monthly Weather Review.

[63] Harsh Rangwani, Sumukh K. Aithal, Mayank Mishra, Arihant Jain, and R. Venkatesh Babu. A Closer Look at Smoothness in Domain Adversarial Training, June 2022. arXiv:2206.08213 [cs].

[64] Pierre Foret, Ariel Kleiner, and Hossein Mobahi. SHARPNESS-AWARE MINIMIZATION FOR EFFICIENTLY IMPROVING GENERALIZATION. In *ICLR*, 2021.

[65] Ying Jin, Ximei Wang, Mingsheng Long, and Jianmin Wang. Minimum Class Confusion for Versatile Domain Adaptation. In Andrea Vedaldi, Horst Bischof, Thomas Brox, and Jan-Michael Frahm, editors, *Computer Vision – ECCV 2020*, Lecture Notes in Computer Science, pages 464–480, Cham, 2020. Springer International Publishing.

[66] Christian Lessmeier, James Kuria Kimotho, Detmar Zimmer, and Walter Sextro. Condition Monitoring of Bearing Damage in Electromechanical Drive Systems by Using Motor Current Signals of Electric Motors: A Benchmark Data Set for Data-Driven Classification. 2016.

[67] Janez Demsar. Statistical Comparisons of Classifiers over Multiple Data Sets. *Journal of Machine Learning Research*, 7:1–30, 2006.

A ECE results for frequency-domain inputs

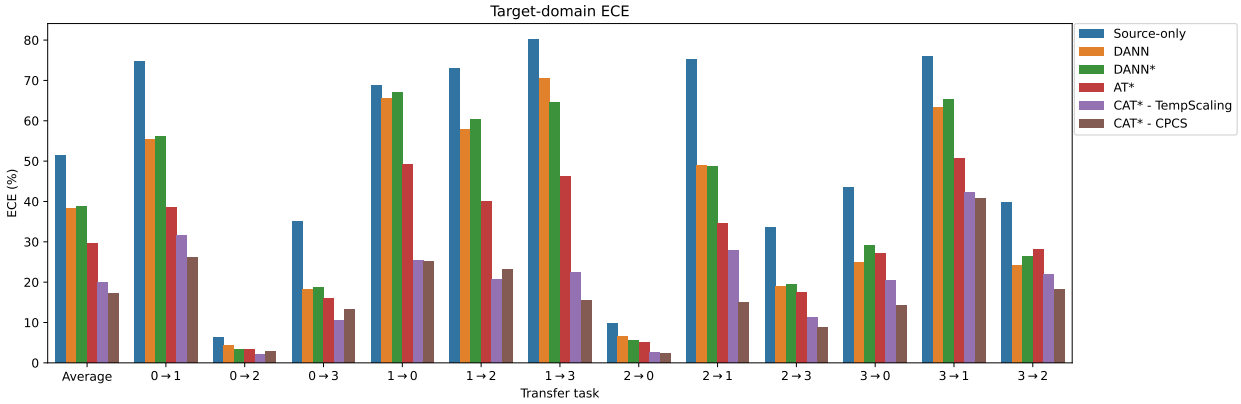

Figure 10: Comparison of target-domain Expected Calibration Error (ECE) for different methods on the PU transfer tasks with frequency-domain input.

Table 10: Target-domain Expected Calibration Error (ECE) on the different PU transfer tasks with frequency-domain input (ECE in %).

Method	$0 \to 1$	$0 \to 2$	$0 \to 3$	$1 \to 0$	$1 \to 2$	$1 \to 3$	$2 \to 0$	$2 \to 1$	$2 \to 3$	$3 \to 0$	$3 \to 1$	$3 \to 2$	Average	Average rank
Source-only	74.82	6.30	35.19	68.69	72.94	80.09	9.85	75.17	33.71	43.62	75.86	39.87	51.34	7.97
DANN	55.48	4.26	18.10	65.55	57.86	70.61	6.58	48.86	19.03	24.96	63.30	24.04	38.22	5.95
DANN*	56.09	3.33	18.61	67.17	60.46	64.68	5.68	48.69	19.48	29.18	65.38	26.45	38.77	6.08
AT*	38.62	3.26	15.92	49.11	40.11	46.12	5.19	34.63	17.49	27.07	50.59	28.04	29.68	4.63
CAT* - TempScaling	31.54	**2.20**	**10.50**	25.46	**20.76**	22.53	2.60	27.88	11.39	20.49	42.23	21.90	19.96	**1.78**
CAT* - CPCS	**26.27**	2.78	13.38	**25.11**	23.21	**15.61**	**2.43**	**15.01**	**8.88**	**14.32**	**40.67**	**18.16**	**17.15**	1.82
CAT* - VectorScaling	39.98	2.46	13.03	32.72	28.85	29.87	3.55	35.00	14.52	23.79	51.84	23.54	24.93	3.03
CAT* - MatrixScaling	42.49	4.09	16.33	39.11	32.10	35.49	5.06	41.30	18.11	27.30	53.45	25.75	28.38	4.73

* = with MCC + SDAT.

B Reliability diagrams for vector and matrix scaling

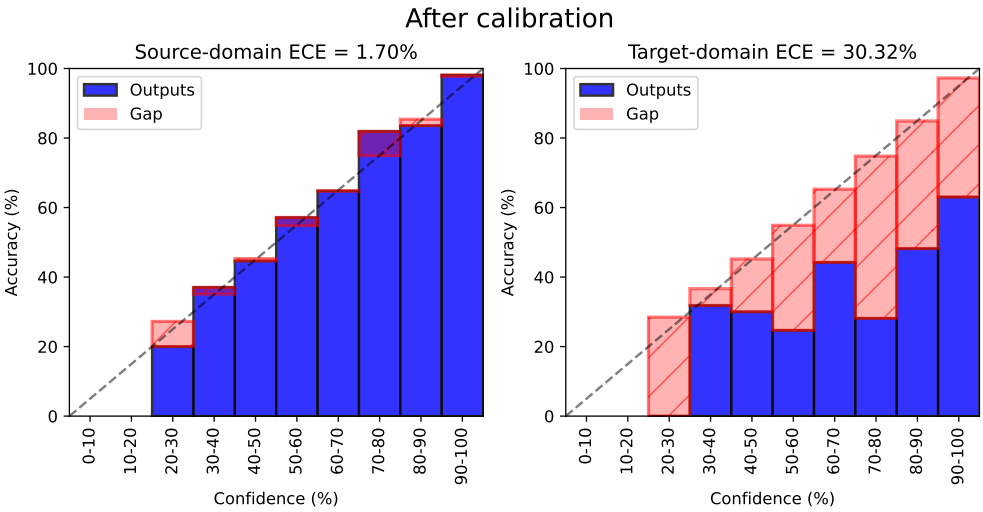

Figure 11: Example of reliability diagram after applying Vector scaling calibration.

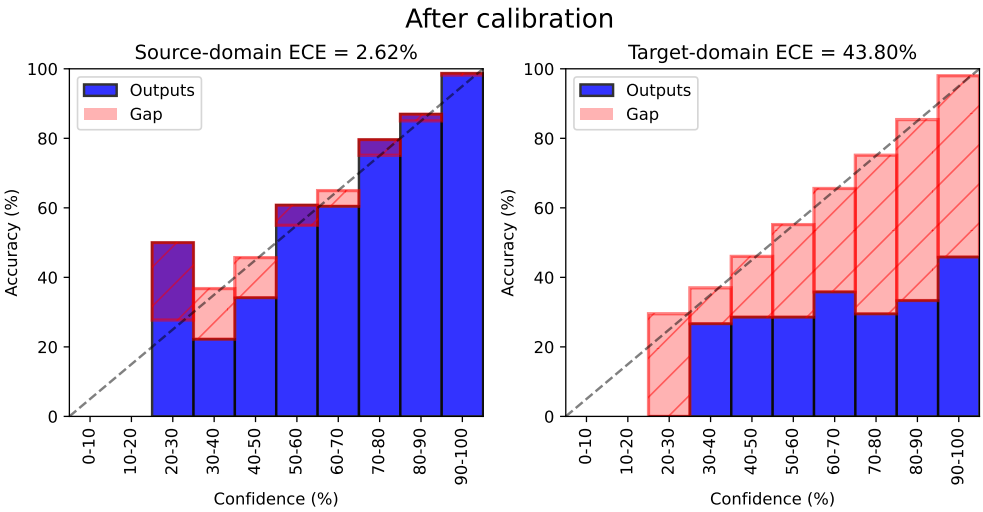

Figure 12: Example of reliability diagram after applying Matrix scaling calibration.

The reliability diagrams shows on Figure 11 and Figure 12 show that the two calibration techniques are able to reduce calibration error more effectively than temperature scaling and CPCS in the source domain. However, in the target domain, calibration error is not reduced. This observation shows that the high number of parameters (scaling matrix and bias vector) of these calibration techniques prevent them from generalizing to the target domain, as opposed to temperature scaling and CPCS which only tune a single scalar parameter on the source test set.